uc3m | Universidad **Carlos III** de Madrid

University Degree in Biomedical Engineering

2017-2018

Bachelor Thesis

"Analysis of the motion of soft animals (Gastropods)"

Andrea Guerrero Campos

Javier Rodríguez Rodríguez

Leganés; September, 2018

ABSTRACT

Terrestrial gastropods crawl by means of a train of pedal waves produced by the contraction and relaxation of the muscles in their ventral foot. The areas between two consecutive pedal waves are known as interwave regions and they remain stationary to the substrate while crawling happens. Adhesive locomotion of terrestrial gastropods involves the secretion of a non-Newtonian yield-stress mucus that communicates the stress of the ventral foot to the ground.

This project puts forward a theoretical model in which the only source of adhesive locomotion is the geometry of the pedal waves, rather than the rheological properties of the mucus. The model is based on the proven existence of small vertical displacements in the ventral surface of terrestrial gastropods and provides a region where any combination of values for the pedal wavelength and the lag between the horizontal and vertical pedal waves allows locomotion to happen. In order to validate this theoretical model, the images taken during a set of experiments performed by Universidad Carlos III in collaboration with the University of California and Stanford University in 2010, have been analyzed through a Digital Particle Image Velocimetry technique. In summary, the aim of this project is to answer the following question: can a biomimetic robot crawl using a Newtonian mucus?

The results show that for three out of the four experiments analyzed, the values obtained fit in the region proposed by the model. Even if three experiments are not conclusive enough to validate the calculations, this project opens the doors to the development of biomimetic robots capable of mimicking terrestrial gastropod's adhesive locomotion using substances exhibiting a Newtonian behavior.

Key words: terrestrial gastropods, Particle Image Velocimetry, Newtonian mucus.

ACKNOWLEDGMENTS

To my two grandmothers, Ángela Rubio and Concepción Cuevas, for providing me with my best memories and being the main reason why I have become who I am.

To my tutor, Javier Rodríguez Rodríguez, for making me part of this project and helping me with the encountered problems.

INDEX OF CONTENTS

INDEX OF FIGURES

CHAPTER 5:

INDEX OF TABLES

1. INTRODUCTION

One of the main goals of biomedical engineering nowadays is the development of devices capable of carrying out surgical/medical procedures as efficient and non-invasive as possible. In order to accomplish this goal, the biomimetic field is gaining strength in its purpose of mimicking biological conditions and properties and take advantage of them in a biomedical context. More in particular, soft biomimetic robots are of special interest in the way that they are capable of performing specific functions not achievable by conventional rigid robots.

One of the biological processes that has been actively studied in the last century is the adhesive locomotion of terrestrial gastropods. At first one can believe that snails and other gastropods crawl too slowly and inefficiently, and thus; that there is little interest in robots trying to emulate them. Nevertheless, there are several advantages that gastropod's crawling has among other locomotion mechanisms. The first one that can be highlighted is the simplicity of a snail's body. The fact that they only have a foot makes them mechanically stable and easy to model. Secondly, terrestrial gastropods have evolved through time in order to travel across many different types of terrains, allowing them to crawl up in vertical surfaces or cross mesh grids. For these reasons among others, the study of gastropod's locomotion together with the latest advances in technology can provide a new wide range of possibilities for biomimetic robots [1].

This thesis offers an insight into the locomotion of terrestrial gastropods and attempts to analyze the small variations of the speed of the ventral foot in the plane perpendicular to the crawling direction. Furthermore, it tries to validate a proposed model for the locomotion of gastropods where they are capable of propelling themselves by means of other substances exhibiting a Newtonian behavior, rather than mucus.

1.1 MOTIVATION

This project was born in 2010 in the minds of 4 researchers passionate about fluid mechanics and its relation to biological processes. One of them was Javier Rodríguez Rodríguez, my thesis tutor; who was capable of transmitting me the same enthusiasm which had taken them to start this set of experiments 8 years ago. What began as a project motivated by curiosity and scientific research, turned out to be an ambitious work which fused physics and fluid mechanics with biological processes that occur spontaneously in nature.

We have all felt the ticklish sensation of a snail crawling along our hand when we were kids, but have we ever thought about what was producing it? This project offered me the possibility of understanding the mechanism behind snail's and slug's locomotion and mathematically describe it the way we have been learning these past 4 years. Moreover, it has made me realize that even behind natural processes that we assume as simple in our daily lives, there is a complex mechanism that up to the date only nature can exactly reproduce.

Apart from the abovementioned reasons, the fact that these biological processes and features can be reproduced in order to develop robots and devices capable having a medical impact on people, made this project even more appealing. Several biomedical applications have aroused from the study of adhesive locomotion. The chances of them being part of the future diagnostic and treatment medical devices are yet unsure, however, what it is clear; is that the understanding and analysis of the biological processes on which they are based must be the first concern that needs to be addressed.

1.2 SCIENTIFIC BACKROUND AND MAIN OBJECTIVES

1.2.1   Some notions of gastropod's adhesive locomotion

Terrestrial gastropods are able to crawl by means of a train of pulses produced by muscle contraction and relaxation. In most terrestrial gastropods, the train of wave pulses is generated in their tails and propagated towards their head (direct waves). However aquatic gastropods exhibit retrograde waves which originate in the head of the animal and propagate towards the tail. The propagation speed of these pulses, commonly known as pedal waves; is usually greater than the overall crawling speed of the animal (2.61±0.44 times greater for garden slugs and 4.54±1.68 for banana slugs [5]). The distance between two consecutive pedal waves is known as the wavelength and it is much greater than the length of the pedal waves. Moreover, the regions in between the waves are called interwaves, and they remain stationary to the substrate in the laboratory reference frame, while locomotion happens. The propagating waves are transmitted to the ground thanks to the mucus secreted by the animal producing a friction force that allows it to slide in a wide range of different surfaces [4]. Hence, the locomotion arises from the combination of the stresses produced within the mucus layer and its fluidic properties. Additionally, the animal's central part of the ventral foot is surrounded by the rim which advances at the same velocity as the animal's center of mass [5].
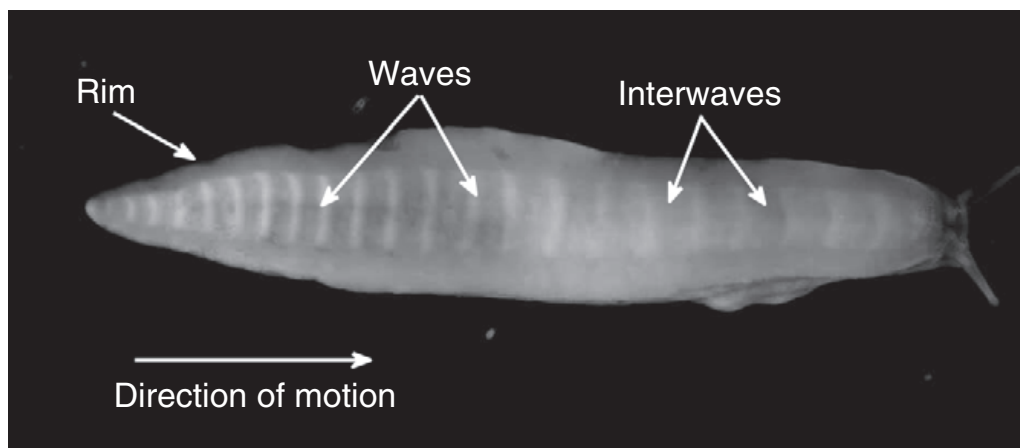
Fig 1.1. *Banana Slug (Ariolimax Californincus) sliding over a transparent substrate from left to right. The train of 23 wave pulses (white) and the interwave regions can be distinguished within the rim. Notice that the interval between two consecutive waves (wavelength) varies as the train of waves propagates from the tail to the head [5].*

1.2.2 First studies about adhesive locomotion

Even if several different models of locomotion for terrestrial gastropods have been proposed, the mechanics of the pedal waves still remains unclear. The first studies classified the train of pedal waves according to their number and direction [6]. According to their direction pedal waves can be direct or retrograde, as mentioned before. However, whether the pedal waves are direct or retrograde, their propagation direction cannot be reversed in terrestrial gastropods, and thus their displacement can only happen in the forward direction. Regarding their number, pedal waves can be monotaxic, if it is just one wave that expands along the whole foot or ditaxic if two pedal waves span the foot [7]. Moreover, later publications have discussed whether the wave's wavelength remains constant or not, concluding that not the wavelength nor their individual speed stays invariant [5].

In 1945, Lissmann was able to prove the stationary nature of the interwaves and showed that the shear stress exerted by the animal's foot on the ground generated a net forward propelling force in the mid-section whereas both the tail and head of the animal produced a sliding friction. Moreover, Lissmann was the first one to postulate that this friction force necessary for the animal's locomotion is a result of its lifting from the ground, by generating a thicker layer of mucus in the pedal wave segments [8].
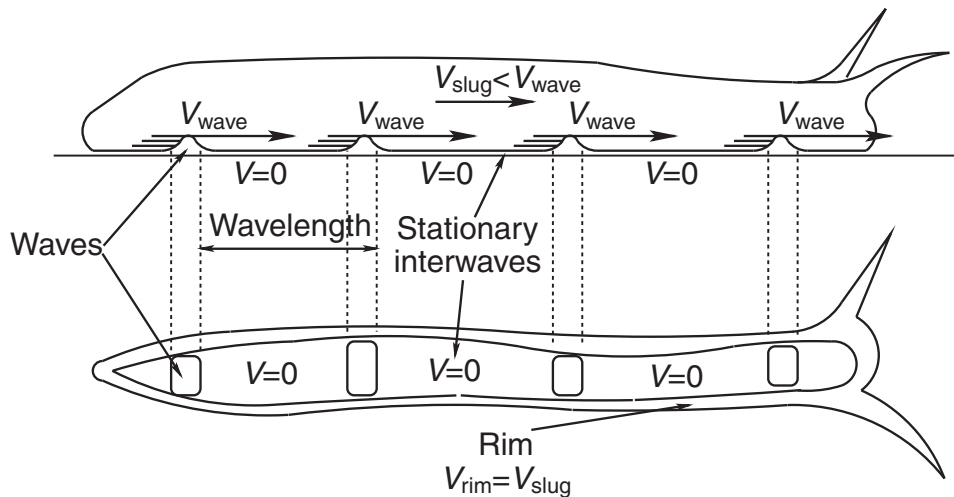
Fig. 1.2. *Outline of the top and bottom views of a terrestrial gastropod where the waves, interwaves and rim can be appreciated. V_{wave} is the velocity of the pedal waves; V is the velocity of the interwaves and it is always equal to zero; V_{slug} is the total crawling velocity of the gastropod and V_{rim} is the velocity of the rim which is equal to V_{slug}. The vertical concavities present in the ventral foot are not to scale. The animal is crawling from left to right. [5]*

1.2.3 Role of the mucus in locomotion

The next great concern affecting gastropod's locomotion is the secretion of mucus and its rheological properties. These characteristics together with the geometry of the waves are thought to be the source of the animal's displacement, but the way that they contribute to the production of thrust and locomotion still remains controversial. However, the only interaction between the animal and the substrate is through the thin mucus layer (usually of the order of ten micrometers thick [7]); hence, locomotion is only made possible thanks to it. Most terrestrial gastropods secrete two different types of mucus: a thick mucus generated by the glands underneath the mouth and a thin mucus layer secreted by the glands underneath the animal's ventral foot [5]. The secretion of mucus accounts for one third of the total energy used by the animal to move, and it is approximately one order of magnitude higher than the total mechanical work needed by the gastropod to crawl [9,10,11]. In a biological context, the mucus is necessary for lubrication and adhesion, as well as for terrestrial gastropods to crawl over inclined surfaces. It is composed of a 95% of water, a small quantity of salts in solution and some glycoproteins of high molecular weight. These proteins when dissolved, create cross-linked networks that provide the mucus its elastic properties [12].

Regarding its behavior as a fluid, the mucus secreted by gastropods can be considered to be a non-Newtonian yield-stress fluid. Subjected under a certain value of the shear stress, the mucus undergoes elastic deformations and behaves as a solid. However, when the yield stress is surpassed, its viscosity drops around 3 orders of magnitude, down to a value which is only 20 times greater than the one of water; allowing the mucus to behave as a viscous fluid [7]. This behavior was first studied in pacific banana slugs (*Ariolimax Columbianus*) by Denny in 1980 and illustrated in Fig.1.3. From the curve it can be observed, that for this sample, the yield strength of the fluid at 0.2% offset equals 17.5 $\times 10^2$ N/m^2 proving that when the pedal mucus is subjected to values of stress lower than this, it behaves as a solid capable of exerting a stress to the substrate.
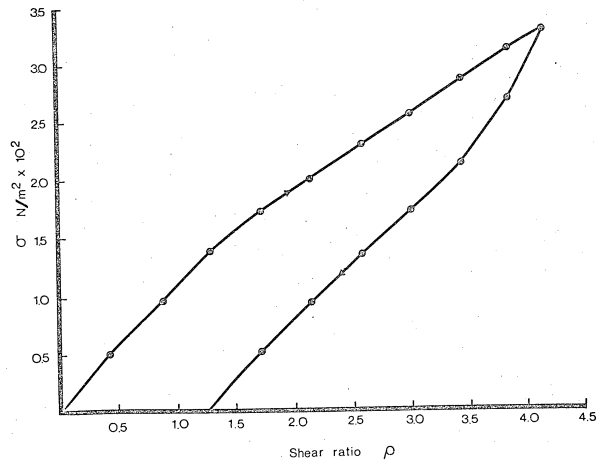
Fig.1.3. Stress/shear ratio curve for pacific banana slug mucus at a moderate shear ratio. Notice that the mucus does not return to its original dimensions [15].

1.2.4 Kinematics of the pedal waves

Regarding the geometry of the pedal waves, it is now well stablished that pedal waves produce concavities in the animal's ventral foot [5]. However, the magnitude of this vertical displacement is 4-10 times smaller than the one of the horizontal displacement, fact that makes the vertical lift of the animal very difficult to measure and evaluate. These concavities where first studied by Parker in 1911 by means of the distortion of air bubbles inside the gastropod's mucus [13]; but it was not until 1973 when Jones confirmed the existence of concavities in the ventral foot by the direct observation of a gastropod which had been frozen while crawling [14]. Later, in 1981; Denny made use of order-of magnitude estimations to put again in doubt the possible existence of these vertical displacements [15]. This controversy was finally solved by the experiments carried out in 2010 by Universidad Carlos III de Madrid in collaboration with the University of California and Stanford University that confirmed physically the existence of vertical displacements in the ventral foot by means of measuring the shear stress underneath the pedal waves and underneath the rim [5].

1.2.5 Dynamics of the pedal waves

In 1981, Denny proved that the viscoelastic properties of the thin mucus were responsible for creating a friction force enough for the animal to propel forward by means of direct pedal waves [15]. Underneath the gastropod's foot, the shear strains fluctuate in time from 0 under the interweaves, and 50 in the segments of biggest displacement [7]. This

way, even if gastropods did not exhibit concavities under their pedal waves, they could be able to crawl forward just relying on the rheological properties of the secreted mucus. This means that in the case that animals remained flat to the substrate, their propulsion would necessarily rely on the finite yield stress of the mucus, which is capable of producing a small stress on the substrate [1]. However, for those animals exhibiting a vertical displacement of the foot, the geometry of their pedal waves would be enough to produce the thrust necessary to travel forward, independently of the rheological properties of the mucus. This way, even if the mucus was substituted by a Newtonian substance unable to produce any stress to the ground, the vertical displacement of the ventral foot would allow locomotion to happen. This fact is the cornerstone of this project: the analysis of vertical displacements in the ventral foot of leopard slugs (*Limax Maximus)* will determine if it is possible to develop a model for adhesive locomotion where the only source of motion relies on the geometry of the pedal waves rather than on the rheology properties of the mucus. In case this model is proven correct, the number of substances that could be used to mimic gastropod's mucus in the biomimetic field will increase and include Newtonian fluids which are easier to model than non-Newtonian ones.

1.2.6 Study which gave origin to this thesis

It was not until 2010, when the experiments on which this thesis is based, answered some additional questions about the kinematics of the pedal waves and their role in the production of traction force. This study concluded that the spatiotemporal distribution of the pedal waves and the interweaves was much more complex than the one accepted before. Up to the date, the pedal waves were considered to be symmetric and to have a constant length and propagation speed. However, the observation of the displacement of the bright speckles on the ventral surface of leopard slugs revealed that the pulse waves deformed and speeded up while travelling from the back to the front of the animal. There were several deformation patterns but the most predominant one was the steady lengthening of the wave followed by its abrupt shortening. This rises the necessity of developing new models that take into account the asymmetry of the pedal waves and their change in velocity [5].

Moreover, these abovementioned experiments performed in 2010, investigated the pulse wave velocity and frequency in comparison with the total crawling speed of the animal during steady locomotion. The fact that the overall crawling speed of the animal and the velocity of the pedal waves are positively correlated had already been accepted, but previous authors had stated this total velocity is only dependent on the frequency and number of waves. Jones stated that faster species exhibit a higher number of pedal waves than slower species [14]. The results proposed in "The mechanics of the adhesive locomotion of terrestrial gastropods" are consistent with the previous hypothesis in which a faster crawling speed corresponds to a higher frequency of the pedal waves. In addition, it was found that the number of pedal waves existing on the ventral surface of the animal decreased as its total crawling speed increased [5]. This way, a smaller number of pulse waves leads to larger area occupied by interwaves and a higher propulsive force. This observation reinforces the fact that the origin of the net propulsive force is underneath the stationary interwaves where the animal remains in touch with the floor and is able to pull its foot backward, compensating the sliding friction caused by the progressing movement of the pulse waves and the animal itself. This can be achieved due to the non-Newtonian yield stress behavior of the mucus which is capable of transmitting the stress produced by the contraction and relaxation of the ventral foot to the ground, creating a point of support that allows the animal to crawl forward.

But probably, the most interesting contribution of these studies for the presented work was to prove the existence of vertical displacements in the ventral foot of slugs. Even if the variation of these displacements could not be measured, their magnitude was evaluated by measuring the points of maximum brightness from two different image bands (one corresponding to a pedal wave region and the other to an interwave region) in a time lapse sequence as follows [5]:
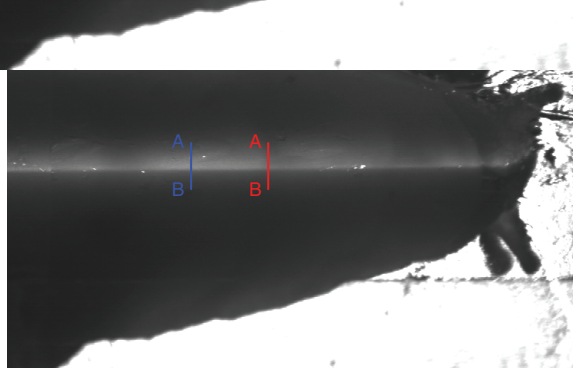
...garden snail while illuminated by a laser sheet. The red and blue bands drawn in the image ...ing the pixels that were correlated. A and B point the origin and end of the lines [5].

...lues of these bands were correlated and fitted into a Gaussian model. ... existence of vertical displacements was the fact that the points of maximum brightness of the two strips did not have the same value, and more important; that their location oscillated passing each other back and forth. This behavior is illustrated in the next figure:
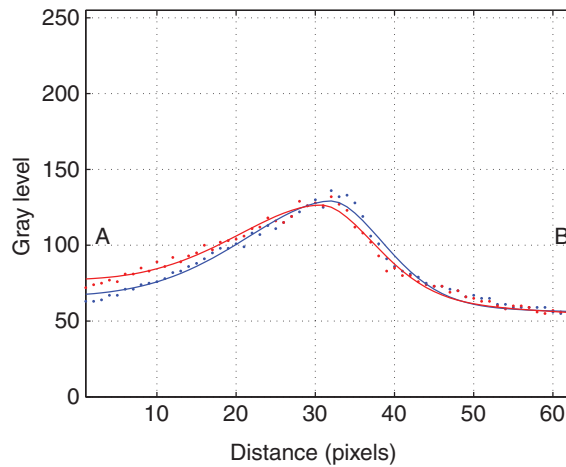
Fig.1.5. Gray-level values fitted into Gaussian curves for the lines depicted in Fig.1.3. Dots represent the real gray-level values whereas the lines reproduce the results when fitted into a Gaussian model.

The relevance of the work carried out in this thesis relies on the abovementioned possibility of gastropods to propel themselves even with fluids exhibiting a Newtonian behavior. However, this can only be achieved with a vertical displacement of their ventral foot, which is significantly small compared to the horizontal displacement and thus, complex to measure and analyze. Even if several authors have observed the concavities

on the ventral foot of gastropods, up to the date there are no experimental measurements of their variation along time and influence on the overall crawling mechanism. This thesis offers the results of the Particle Image Velocimetry analysis of the vertical displacement of gastropods' foot in order to validate the proposed mathematical model that would allow terrestrial gastropods to crawl forward independently of the rheological properties of their secreted mucus.

1.3 POTENTIAL APPLICATIONS IN THE BIOMEDICAL FIELD

What increases the appealing character of this work are its potential applications in the biomedical field, especially in the development of biomimetic robots. Terrestrial gastropods, unlike many other terrestrial species that walk on their legs with discrete contact to the ground; use the whole ventral surface of their foot to crawl smoothly over the substrate. This allows them to move in all types of terrains including vertical surfaces or the sharp end of a knife. The possibility of building robots capable of propelling themselves by means of directional waves provides them the ability to move within curved and narrow spaces and crawl over rough terrains while adsorb to the ground.

With this motivation in mind, there have been several research groups which have pursued building actuators based on adhesive locomotion. Based on the observed wave patterns followed by gastropods while travelling, the Tokyo Institute of Technology (Japan) developed an actuator divided in various segments which are capable of generating a travelling wave by means of supplying different pneumatic pressures. Results showed that the generated wave has large amplitude and moving capacity, being able to carry heavy objects (up to 300g) [18]. Moreover, this same technology has been broadened in order to build omni-directional locomotion systems using traveling waves propagation [19].   This technology taken to its state of art could be applied for the locomotion systems in exploration robots and even in wheelchairs and walkers that could travel across surfaces where wheels would fail to.

However, the biomedical application of these actuators that is closest to become possible in the next years is related to endoscopic imaging. Endoscope technology has not stopped

gaining relevance since its first appearance in the nineteenth century which is explained by the increasing number of digestive diseases, especially cancers in the gastrointestinal tract [2]. However, conventional endoscopes are not always capable of correctly detecting the disease in the gastrointestinal tract due to large distances existing from the orifice to the point of interest. Capsule endoscopes were developed in order to solve this complication. Despite their many benefits, capsule endoscopes have some limitations since they cannot move actively along the gastrointestinal tract but are subjected to peristaltic movements. Late approaches have tried to develop capsule endoscopes that include a propulsion system based on the motion of terrestrial gastropods, so that they are able to stick and travel along the walls of the tract without harming it. The department of Bioengineering Robotics of Tohoku University (Japan), has designed a prototype crawler which is able to travel along rubber plates and climb sloped surfaces covered by mucus. This capsule endoscope based on snail motion takes advantage of the friction between itself and the inner walls of the digestive tract, to move along it in any direction despite gravity [3].

The potential of biomimetic robots based on natural physical properties in medical procedures is of high concern and thus, the analysis and understanding of these characteristics is the first step that needs to be addressed.

1.4 STATE OF THE ART

Based on the studies described in the paper "The mechanics of the adhesive locomotion of terrestrial gastropods', written by Janice H. Lai, Juan C. del Alamo, Javier Rodríguez Rodríguez and Juan C. Lasheras and published in 2010; several research groups have developed and proposed different mathematical models to describe snail's and slug's locomotion mechanisms. Some of these more recent studies focus on the kinematics and types of the pedal waves whereas others pay attention to the mechanical properties of the mucus in relation with the overall crawling mechanism.

In 2013, the California State University Long Beach (California, USA) in collaboration with the University of Scranton (Pennsylvania, USA) analyzed the gait of terrestrial

gastropods concluding that some of them can crawl using two different mechanisms: adhesive crawling and loping. In the first method, the complete ventral foot of the animal is separated from the substrate just by a mucus layer and the animal leaves an uninterrupted mucus trail. On the other hand, loping involves the arching of some regions of the animal's foot so that the left trail is discontinuous. Loping waves appear in addition to the pedal waves. It is believed that loping is implemented by terrestrial gastropods when rapidly trying to escape from predators. Besides, the choice between adhesive locomotion or loping depends on the substrate on which the animal is crawling: garden slugs (*Helix Aspersa*) use adhesive locomotion while crawling on acrylic surfaces and loping on concrete surfaces. Furthermore, they proved that snails moving on concrete secreted higher volumes of mucus than the ones moving on acrylic surfaces by adhesive locomotion [27].

One year later, in 2014, a paper explaining the advantages of mucus for adhesive locomotion in terrestrial gastropods was published in the Journal of Theoretical Biology. Its main contribution was the study of the hysteresis properties of the mucus, that together with the contraction ratio of the muscles in the ventral foot, was proved to be essential in the regulation of kinetic friction. A mathematical model was proposed based on the assumption that the hysteresis properties of the mucus are the main features that allow propagation of both direct and retrograde pedal waves [28].

2. THEORETICAL MODEL

Since the first studies, the non-Newtonian nature of terrestrial gastropods' secreted mucus has been well established. As previously mentioned, this mucus can be modelled as a shear-thinning fluid which behaves as an elastic solid under a so-called yield stress, but is able to flow like a viscous liquid when this value is surpassed. The prior studies developed by Universidad Carlos III de Madrid in collaboration with the University of California San Diego (UCSD) and Stanford University attempted to reveal up to what extent does the rheological properties of terrestrial gastropods' mucus are essential for locomotion. Would terrestrial gastropods be able to propel themselves forward even if their mucus did behave as a Newtonian fluid? The answer to this question is critical in the biomimetic field for those who put their efforts on engineering and developing devices emulating the locomotion of gastropods. The possibility of building a model that does not rely on the non-Newtonian properties of the mucus increases the number of different fluids that could be used in order to mimic the role of the gastropods' mucus.

The proposed model tries to clarify if the relation between the pedal wavelength and the lag between the vertical and horizontal displacement functions of the ventral foot is significant enough to be the only source of adhesive locomotion. For this purpose, it provides a region of possible values for these two parameters where locomotion can happen. Thus, for every combination of values fitting in this region, the geometry of the pedal waves would be enough to produce motion by itself, without being influenced by the fluidic properties of the mucus. Moreover, it introduces a slip velocity under the interwave regions of the animal's foot (that no longer remain stationary to the ground) which is of smaller order of magnitude than the pedal wave velocity. This slip velocity is necessary for locomotion to happen when the fluid mimicking mucus exhibits a Newtonian behavior, since it cannot longer exert a stress to the ground as the finite yield stress non-Newtonian mucus.

In order to start assessing the model, let us consider a fluid film flowing in between a flat stationary surface (the ground) and another surface with the property of deforming in both horizontal and vertical directions (the animal's foot). The foot can be considered as a

surface moving at constant horizontal speed $Uf(x, t)$ and governed by the following equation:

$$y - h(x, t) = 0$$

[1]

At this point is possible to sketch the model and define the main parameters as follows:
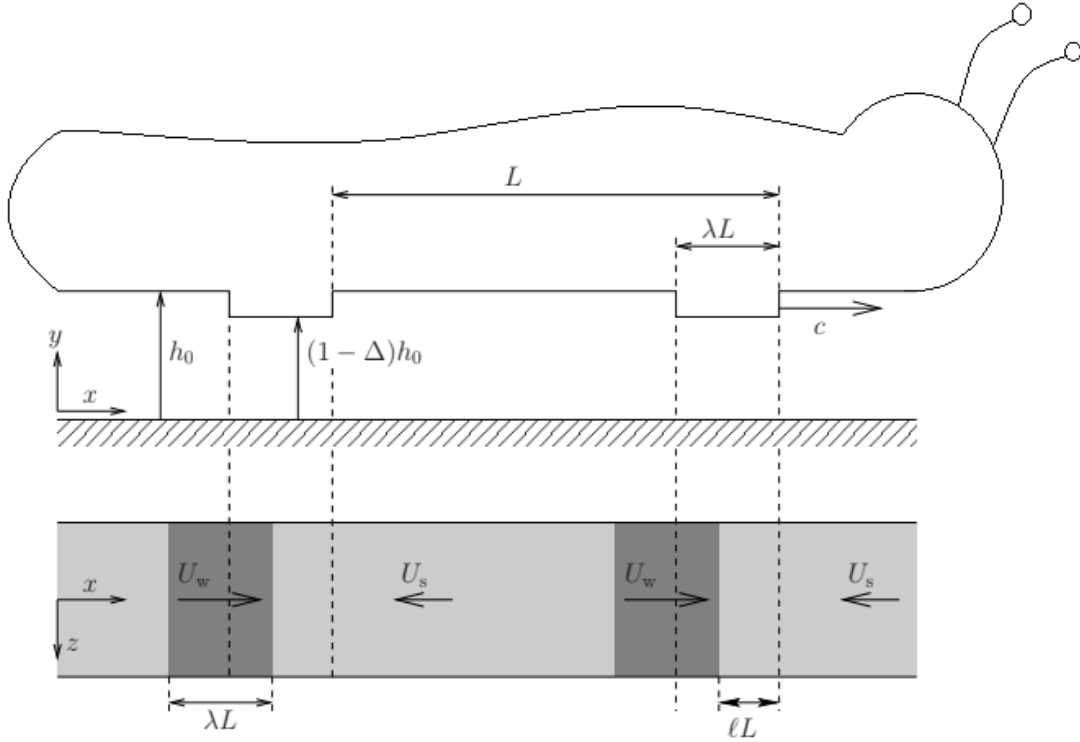
Fig. 2.1. *Sketch of the geometry of the model proposed in the simplified case of a square deformation wave. The animal is crawling from left to right.*

Both the horizontal and vertical displacements are considered to follow a train of waves pattern defined by its propagation speed, c and wavelength L. Hence it is necessary to define the vertical and horizontal deformation waves for the animal's foot. If ξ is the phase of the pedal wave and equals to $\xi = \omega t - xt$, then $g(\xi)$ and $f(\xi)$ are the deformation functions in the horizontal and vertical axes respectively depending of the wave's phase. To avoid complications, these deformation functions will be considered to be square waves with same shape and factor λ (or pedal wavelength), but with a difference of phase of $\xi=2\pi l$ (l being the lag) between them. These assumptions are based on the experimental observation of a delay between the horizontal and vertical pedal waves that will be illustrated during the description of the results.

14

$$f(\xi) = g(\xi + 2\pi\ell) = \begin{cases} 0, & 0 < \xi < 2\pi(1-\lambda) \\ 1, & 2\pi(1-\lambda) < \xi < 2\pi \end{cases} \quad \text{[2]}$$
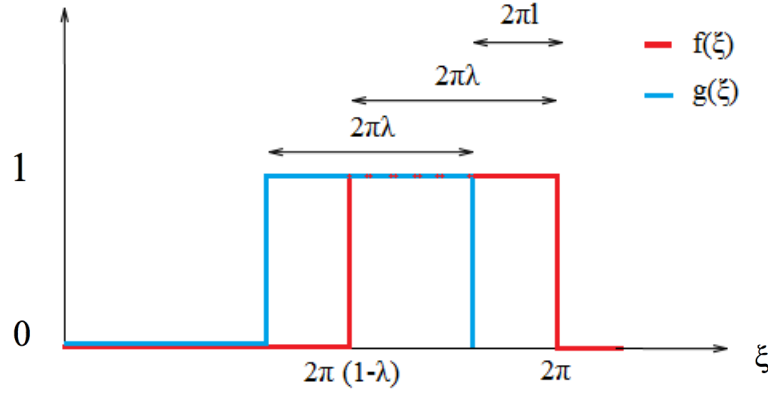
Fig.2.2. *Plot of the assumed deformation functions in the vertical (red) and horizontal (blue) axes.*

Under these conditions the equations modeling the gap thickness **h(x, t)** and horizontal velocity of the foot U_f**(x, t)** are shown below:

$$h(x,t) \quad = \quad h_0\left(1 - \Delta f(\xi)\right) \quad \text{[3]}$$

$$U_f(x,t) \quad = \quad U_s + (U_w - U_s)\, g(\xi) \quad \text{[4]}$$

where **h0** is defined as the thickness of the gap during an interwave, U_w is the maximum horizontal speed of the foot (at the pedal wave) and U_s is the velocity outside the region of maximum velocity, commonly known as slip velocity (velocity arising from the friction force).

Moreover, due to the geometry of the model under study, the lubrication theory can be applied. The lubrication theory applies when the fluids gap thickness is much smaller than the other length scale. In our model, the gap thickness, **h(x,t);** is considerably small compared to the scale of the wavelength **(L),** that is, $h_0/L \ll 1$, $\omega h_0^2/\nu \ll 1$ and $(U_w h_0/\nu)\cdot(h_0/L) \ll 1$. At this point, the formulas derived from the mass and momentum conservation equations which mimic the flow in the gap will be:

15

$$0 = \partial_x u + \partial_y v \tag{5}$$

$$0 = -\partial_x p + \mu \partial_y^2 u \tag{6}$$

The following boundary conditions must be considered in order to solve the previous equations:

$$u = v = 0 \quad \text{at} \quad y = 0 \tag{7}$$

$$u = U_\text{f}, \; v = \frac{\mathrm{d}h}{\mathrm{d}t} = -\omega \frac{\mathrm{d}h}{\mathrm{d}\xi} = \omega \Delta h_0 f' \quad \text{at} \quad y = h(x,t) \tag{8}$$

Regarding the previous boundary conditions, it is relevant to highlight the simplification of considering the pressure gradient equal to zero inside the fluid gap. This decision has been taken based on the fact that gastropods are able to crawl on top of mesh grids of very thin parallel threads, which are placed at a distance higher than the pedal wave's wavelength. Under room conditions the pressure is equal to the atmospheric one and remains constant, without leading to a variation in their pattern or frequency. From this fact, it can be assumed that the pressure gradient does not play a critical role in gastropods' locomotion. Additionally, as the desired solution is periodic over time, no initial conditions need to be addressed in order to solve the equations describing the model.

After applying the aforementioned conditions to the equations, we obtain a simple solution for the horizontal velocity profile:

$$u = U_\text{f} \frac{y}{h} \tag{9}$$

Furthermore, relying on the absence of pressure gradient of the gap, the horizontal stress exerted by the fluid on the foot will be given by:

$$\tau = -\mu \left. \partial_y u \right|_{y=h} = -\mu U_\text{f}/h \tag{10}$$

On the other hand, the traction force is defined as the integral of the shear stress along one wavelength on the foot and it can be derived as follows:

16

$$T = -\mu \int_0^L U_{\mathrm{f}}/h \, \mathrm{d}x.$$

[11]

Where **L=2π/L.** Substituting U_{f} for equation [5] and making a change of reference knowing that

$$\xi = kx - \omega t; \, dx = \frac{d\xi}{k}$$

[12]

We arrive at the following formula for the traction force at the foot of the animal:

$$T = -\frac{\mu U_{\mathrm{w}}}{h_0 k} \left[u_{\mathrm{s}} \int_0^{2\pi} \frac{\mathrm{d}\xi}{1 - \Delta f} + (1 - u_{\mathrm{s}}) \int_0^{2\pi} \frac{g \, \mathrm{d}\xi}{1 - \Delta f} \right]$$

[13]

Where **u$_s$=U$_s$/U$_w$** is the velocity of the foot at the interwave made dimensionless with the velocity at the pedal wave.

As stated before, the deformation functions will be simplified as square waves in order to adopt a simple model that illustrates the physics of the locomotive mechanism. This way, in a square waves approximation, by substituting the functions of *g(ξ)* and *f(ξ)* in equation [13] the following expression for the total traction force along a wavelength is obtained:

$$T = u_{\mathrm{s}} \left(1 - \lambda + \ell \frac{\Delta}{1 - \Delta} \right) + \frac{\lambda - \ell \Delta}{1 - \Delta}$$

[14]

In order to fulfill the first Newton's Law when the animal is sliding with a constant center-of-mass speed, the total traction force must be equal to zero yielding the next equation for the ratio of the foot velocities:

$$u_{\mathrm{s}} = -\frac{\lambda - \ell \Delta}{(1 - \lambda)(1 - \Delta) + \ell \Delta}$$

[15]

It is relevant to highlight that since **Δ<1** and **l< λ<1,** the velocity at the interwave **U$_s$** must have an opposite sign to the velocity at the pedal wave for the net traction to be zero. This velocity is known as the ''slip velocity'' of the foot at the interwave and it is the speed which arises from the friction caused by the animal's body moving in the forward direction. From this, it can be easily observed that for locomotion to happen when mucus is substituted by a Newtonian substance, the interwave regions of the ventral foot cannot

17

remain completely stationary to the substrate. There must be a small velocity that compensates the fact that Newtonian substances cannot produce stress on the underlying surface.

Furthermore, in the approach to prove that terrestrial gastropods are able to crawl forward independently of the rheology properties of their mucus, it is interesting to point out that the magnitude of the shear stress under the interwave $\tau_{s,}$ is |u_s|(1-Δ) times smaller than the stress under the pedal wave τ_w. Following this line of thought, it would be possible for the animal to take advantage of the mucus' non-Newtonian rheology to eliminate the slip velocity provided that the mucus' yield-stress, τ_y fulfills the following condition:

$$|u_{\mathrm{s}}| \left(1 - \Delta\right)\tau_{\mathrm{w}} < \tau_{\mathrm{y}} < \tau_{\mathrm{w}}.$$
[16]

Therefore, the model proposed allows the animal to move even when the mucus is Newtonian. This way in order to prove that a net forward force can be achieved despite the existence of the slip velocity, the net volume V of the body that passes through a vertical control surface during a wave period $2\pi/\omega$ will be calculated assuming that the animal has a unit cross section that horizontally moves at the same time as the foot underneath:

$$V = \int_0^{2\pi/\omega} U_{\mathrm{f}}\, \mathrm{d}t = \frac{U_{\mathrm{w}}L}{c}\left(\lambda + u_{\mathrm{s}}\left(1 - \lambda\right)\right)$$
[17]

substituting the expression for the dimensionless interwave velocity u_s:

$$V = \frac{U_{\mathrm{w}}L}{c}\frac{\Delta\left(\ell - \lambda\left(1 - \lambda\right)\right)}{(1 - \lambda)(1 - \Delta) + \ell\Delta}$$
[18]

Thus, a center of mass velocity $U_{c.m}$ can be defined as the average of volume that crosses the section during one period:

$$U_{\mathrm{c.m.}} = U_{\mathrm{w}}\frac{\Delta\left(\ell - \lambda\left(1 - \lambda\right)\right)}{(1 - \lambda)(1 - \Delta) + \ell\Delta}$$
[19]

For forward locomotion to happen, the center of mass velocity $U_{c.m}$ must be greater than zero. Since the denominator of equation [20] will always be positive, the only way $U_{c.m}$ is positive as well is that the following inequality is fulfilled:

18

$$\ell > \lambda\left(1 - \lambda\right)$$

[20]

Moreover, it has experimentally been proved that both the vertical and horizontal displacement waves corresponding to the same pedal wave must overlap [5]. Inequality [20] together with this condition, that can be described by the following inequality:

$$\ell < \lambda$$

[21]

yield a region of possible lags between both waves that allow the animal to crawl forwards. The shaded area of Fig.2.3 represents the area bounded by the inequalities [20] and [21] in which the gastropod can undergo a net forward motion for a given pedal wave length:
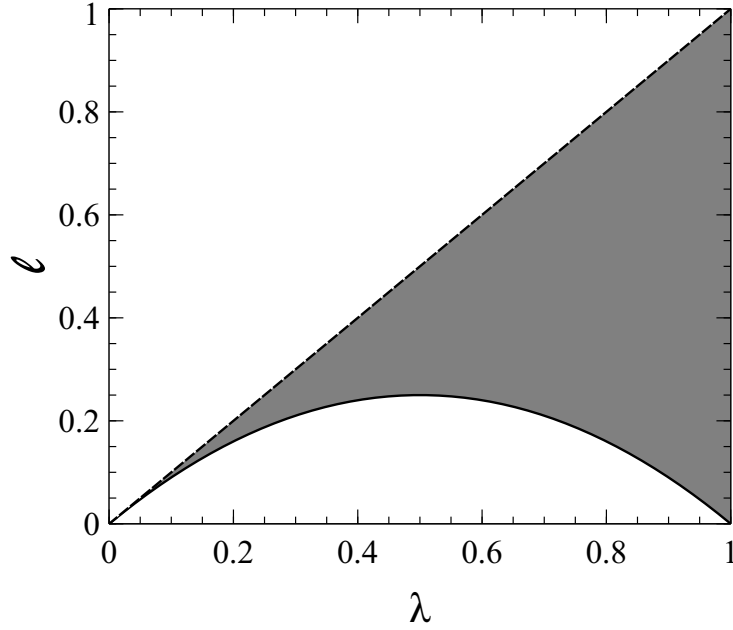
Fig. 2.3. Inequality [20] together with the condition that the horizontal and vertical deformation waves must partially overlap (l<λ), restrict the possible values of the lag, l that allow the gastropod to undergo a net forward motion for a given pedal wavelength λ (shaded area).

Finally, it is essential to prove that the model preserves the length of the animal during locomotion. This way, in order to generalize the model for every deformation function taken, the only assumption made will be the 2π periodic nature of *g(ξ).* Hence, considering the body to be a compressible fluid and assuming that the only movement in the vertical direction is the one related to the foot's lift associated to the pedal wave, the

volume of body generated per unit time and unit volume will be the divergence of the body's velocity field v_f:

$$\frac{1}{\mathcal{V}}\frac{\mathrm{d}\mathcal{V}}{\mathrm{d}t} = \nabla \cdot \vec{v}_{\mathrm{f}} = \partial_x U_{\mathrm{f}} = (U_{\mathrm{w}} - U_{\mathrm{s}})\,kg'$$

[23]

Thus, the net generation of body volume along a wavelength, at a fixed time, is:

$$\int_0^L \frac{1}{\mathcal{V}}\frac{\mathrm{d}\mathcal{V}}{\mathrm{d}t}\,\mathrm{d}x = (U_{\mathrm{w}} - U_{\mathrm{s}})\int_0^{2\pi} g'\,\mathrm{d}\xi = 0.$$

[24]

The last integral is equal to zero due to the periodic nature of *g(ξ)*. Moreover, it is interesting to highlight that this conclusion is also valid for real situations where the velocity of the animal's foot does not only change in the axial direction of the body but also perpendicular to the symmetry plane. To illustrate this point, Fig.1.5. displays the instantaneous realization of the divergence of the foot's velocity field. It can be easily observed that regions of expansion of the foot (red) and contraction regions (blue) exhibit nearly the same form and intensity and thus, they cancel each other. The contraction is associated to the front of the pedal wave whereas the expansion is related to the muscular relaxation that takes place after the wave has passed.
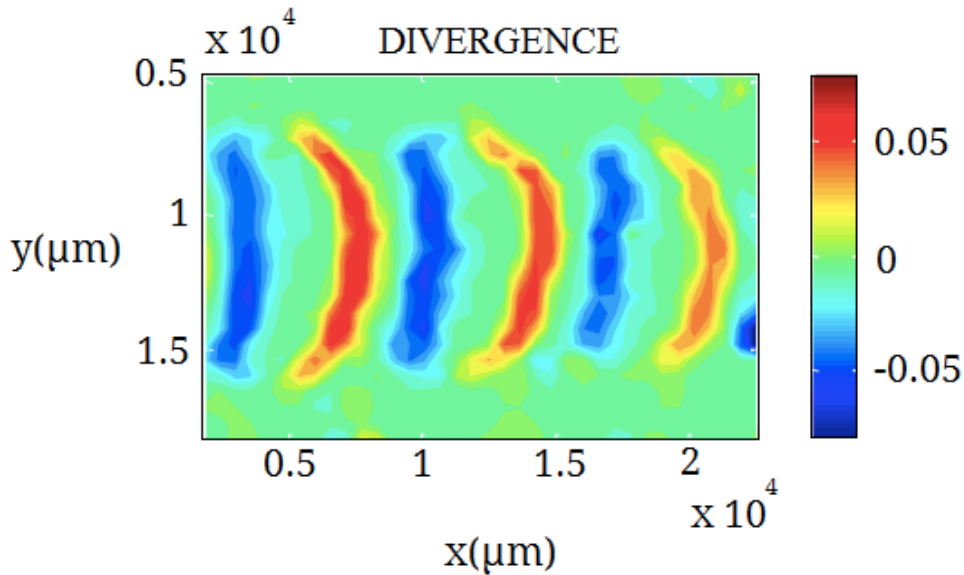
Fig.2.4. *Instantaneous divergence of the foot velocity field (div(**vf**)). Red regions indicate expansion of the foot areas whereas blue regions point out contraction. Despite the existence of local contraction/expansion areas, the periodic nature of the deformation function guarantees that the total volume of the animal is preserved during locomotion.*

3. MATERIALS AND METHODS

3.1 SET OF EXPERIMENTS CARRIED OUT

The presented thesis is based on a series of experiments carried out in 2010 in San Diego, CA, USA by Janice H. Lai, Juan C. del Alamo, Javier Rodríguez Rodríguez and Juan C. Lasheras; and described in "The mechanics of adhesive locomotion of terrestrial gastropods". The measurements were obtained from the observed deformation produced by the animals as they slide along substrates of known elastic properties [16]. The layout of the lasers and cameras allows the measurement of the exerted horizontal stresses not only around the animal, but underneath its surface.

Two sets of experiments were performed in order to measure the kinematics and dynamics of the pedal waves. The study presented in this thesis is focused just on the kinematic measurements which try to clarify the mechanism which makes adhesive locomotion possible.

Two different species were used to carry out the procedures: gray garden slugs (*Deroceras Reticulatum*) and garden snails (*Helix Aspersa*). These two species of gastropods were selected for the experiments because even if they are originally from Europe, they can be found in every country except the Antarctica in such great amounts that they are usually considered as a pest. However, the images that this thesis has analyzed come from another set of experiments that repeated the same procedure for other two species of leopard slugs (*Limax Maximus*), taking advantage of the bright/white speckles present on their ventral surface for image analysis purposes. Leopard slugs are originally European terrestrial gastropods which can measure up to 10-20 cm and have a light greyish or grey-brown body spread with dark spots. The reason why the experiments were repeated with this species is just the possibility of using their bright speckles (do not confuse with the dark spots spread over their skin) as tracer particles for the Particle Image Velocimetry technique. The raw data used in this thesis corresponds to the experiments done with leopard slugs. The procedures were performed at constant room temperature and the mass of the animals was kept constant through the whole experiment.

Fig.3.1. *Leopard slug (Limax Maximus). The dark speckles present in its body are used as tracer particles in the Particle Image Velocimetry analysis.*

In the set of experiments which tried to assess the kinematics of the locomotion, the gastropods crawled along a flat horizontal transparent surface which allowed the visualization of the ventral foot of the animal when properly illuminated with a laser sheet. Keeping a rate of 15 frames per second for 3 to 6 seconds, different series of 1024x1024 gray-level images where obtained. For analysis purposes, the velocity of the center of mass of the subjects was measured and only images belonging to the motion at constant speed and direction were kept as valid.
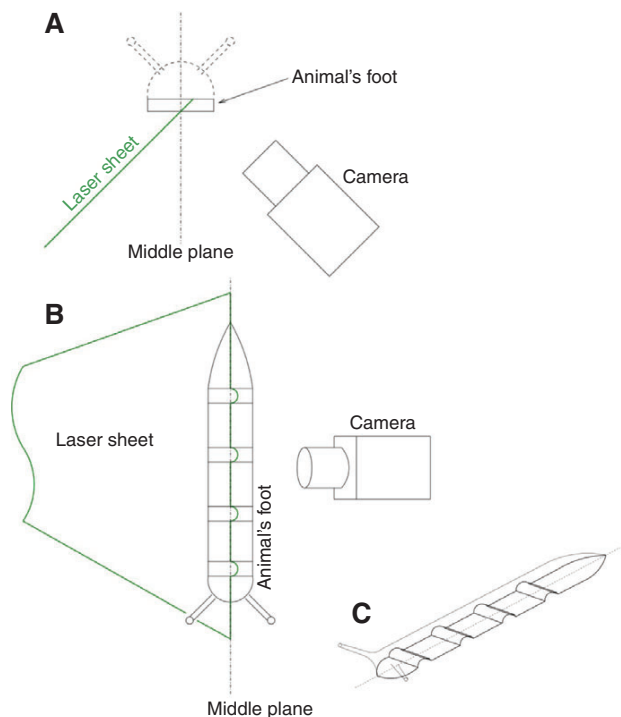
Fig.3.2. *(A) Front prospect of the experimental outline. The animal crawls out of the page. (B) Top prospect of the experimental outline. The gastropod is seen from above. (C) 3D sketch of the animal [5].*

The key of the experiments for this thesis was the possibility of measuring the vertical displacement of the ventral foot of the animals associated with the passage of the pedal wave. For that purpose, the laser was mounted in order to illuminate the ventral foot of the gastropod forming a finite angle with its vertical middle plane. This way, if the foot remained flat to the surface, the intersection between the animal and the laser would yield a straight line visible in any camera view. However, if the ventral foot suffered from some arching, the intersection line will exhibit some deviations. The projection of these deviations in the image is proportional to the vertical displacement of the foot with respect to the substrate. Finally, in order to obtain the calibration factor (um of vertical displacement per pixel of the image), an image of a block with some notches of known depth was taken without changing the experimental set up [5]. However, the curvature of the interference line was not visible to the naked eye because the vertical displacement is really small compared to the magnitude of the laser sheet. In order to quantify the deviations, this thesis will try to measure the displacement of the bright particles of the ventral foot between every consecutive image of the lapse sequence by means of the Particle Image Velocimetry technique.

The analysis carried out in this thesis will use 4 out of the 8 the experiments performed with leopard slugs, that have a variable number of images within the range of 160 and 200.
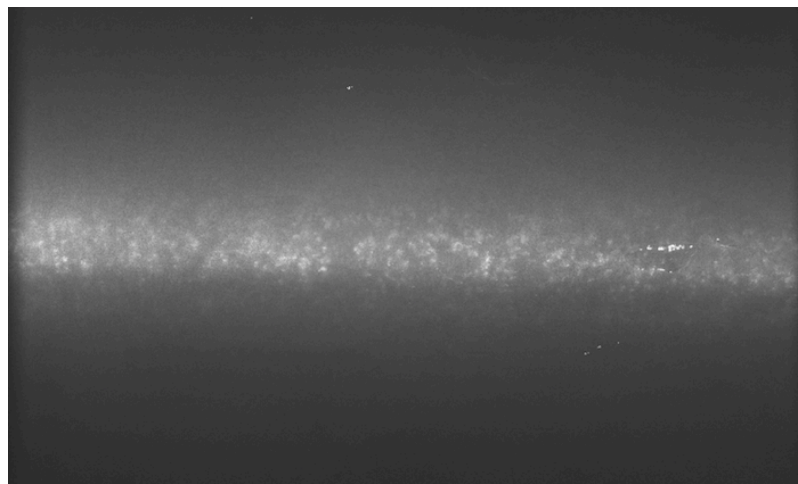
Fig.3.3. Output of the aforementioned experiments. The incidence of the laser with body of the leopard slug allows the observation of the bright speckles of its ventral surface. The ventral foot is seen from below through a transparent surface over which the animal is crawling.

3.2 DIGITAL PARTICLE IMAGE VELOCIMETRY TECHNIQUE

Digital Particle Image Velocimetry (PIV) is a technique that allows to obtain an instantaneous velocity field of a fluid both in liquid and gaseous state. The final goal is achieved by including tracer particles within the fluid which acquire the same velocity as the flow in which they are embedded. However, in the experiments with leopard slugs, there was no need of introducing additional tracer particles since these animals have bright speckles on their foot's skin that can be used as natural tracers. Additionally, a laser is mounted and placed in such way that together with a lens and the liquid holder, is capable of producing a thin sheet of light in the desired plane and illuminate the tracer particles in the fluid.

Consequently, the tracer particles scatter the laser's light which is then detected by a CCD o CMOS sensor in frames separated by a short-known time interval. This way, two images are obtained where two different positions of the same group of particles can be observed. From them, their velocity vector can be calculated from the quotient between the displacement and the time interval [17].

Thereafter the frames are analyzed in a computer. Two sequential frames are sub-sampled in a specific region by means of interrogation windows. Within these windows the particles suffer a spatial shift that can afterwards be measured. The spatial shift can be understood as the response of a system where the input is the sampled region of one image, and the output is the sampled region of another image taken Δt time after (Δt known as the temporal increment). Moreover, the system includes an additive noise function which arises from the particles moving out of the sampled region or disappearing due to the 3D motion [23]. The computation of the spatial shift is usually performed by statistical methods such as the auto-correlation and the cross-correlation. This analysis allows to obtain the local displacement vector of the tracer particles, that can be studied and analyzed subsequently.

3.3 WORKFLOW OF THE ANALYSIS

The kinematic assay that is to be explained below is based on PIVlab and several MATLAB implementations. PIVlab is a digital image particle velocimetry tool which allows the calculation of the velocity distribution within various image pairs. It is based on multi-pass cross correlations which applies a standard cross correlation in the first step and then shifts the interrogation window of the second image taking into account the displacement vector obtained in the previous standard cross-correlation. This way, the displacement obtained is lower at each iteration until it becomes nearly zero. The final displacement vector will be the sum of all the previous displacements. PIVlab also includes multi-grid cross correlation which reduces the window size at each iteration of the multi-pass process. This allows a higher spatial resolution and a wider dynamic velocity range (DVR) [24]. Additionally, it provides the options of selecting a specific window size as well as a Region of Interest which will be determine the quality of the results obtained. PIVlab software was chosen for this analysis since it provides the option of exporting several parameters of the flow analysis into MATLAB files.

It is necessary to highlight that for our purpose it is more convenient to work without physical magnitudes. The whole spatiotemporal analysis is carried out and discussed in pixels and frames units since the goal is to obtain good quality of the signals rather than physical magnitudes. This way, good results will be obtained when the signal has a larger variation than the unit pixel. The results will only be converted into physical magnitudes when they need to be compared and validated with values described in other studies. For reference purposes, the spatial and temporal scale will be provided.

3.3.1 Velocity Analysis

In the first instance, it was necessary for the raw images provided to undergo a preprocessing procedure. Each image was rotated 90º clockwise in order for the horizontal axis to match with the displacement of the animal and the vertical one with its lifting in the vertical direction. Moreover, the images were subjected to some preprocessing features included by PIVlab such as contrast enhancement and intensity capping, that minimizes the error introduced by the presence of other bright particles in the image rather than the tracer particles.

25

The proposed model assumes that both the horizontal and vertical displacement functions of the ventral foot follow a wave pattern. Hence, the initial purpose was to prove their periodic behavior. As mentioned before, the displacement of the slug's ventral foot in the vertical direction is commonly much lower than the one in the horizontal direction. This fact makes the vertical displacement really complex to measure, up to the point that nearly any experiments carried out with this purpose have manage to accomplish it. In the analysis performed in this thesis, all the efforts were focused on trying to observe a wave pattern in the vertical direction and extract its wavelength in order to set some values for which locomotion is possible and check whether they fit in the proposed model.

Once the images had been adapted to the needs of the analysis, they were loaded to PIVlab to start the evaluation. At first, several different window sizes were used in order to find the ones that provided the best results. The ultimate chosen window size was 64x32 pixels. With the aim of avoiding the calculation of misleading or empty velocity vectors in darker regions of the images, they were ultimately removed and interpolated making use of the vector validation option provided by the PIVlab tool.
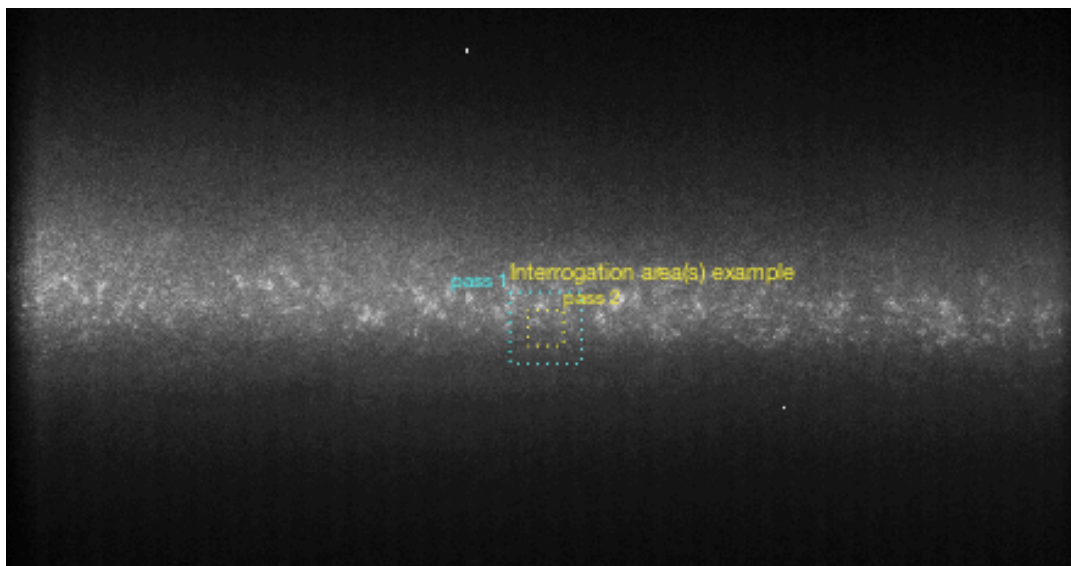
Fig.3.4. Illustration of the size of the selected interrogation window in comparison with the magnitude of the ventral foot of a leopard slug.

The output PIVlab session, including the all the velocity vectors; was loaded to a MATLAB script in the effort of filtering them once again, this time by modulus and by

selecting a more accurate Region of Interest. The instantaneous velocity field was averaged across the light image band in order to obtain the instantaneous velocity vector for both horizontal and vertical axis. Even if the data coming from noise was reduced, at this point; the velocity vectors in the vertical direction did not show a clear periodicity. In order to prove this, the velocity vectors in both directions were circularly auto correlated. Autocorrelation is the cross correlation of a signal with a delayed copy of itself as a function of its delay. It provides information about the similarity between patterns as a function of their lag and thus, it is an effective tool to measure the periodicity of a signal. For our purpose, the circular cross autocorrelation, where the vector **f** is circularly shifted by **k** samples; was implemented as follows:

$$C(k) = \frac{1}{N} \sum_{n=0}^{N} f(n) \times f(n-k)$$

[25]

The final aim of the analysis is to obtain a value for the wavelength of both horizontal and vertical displacement patterns, which must be the same; and a value for the lag between both functions. At this point of the analysis, this goal could not yet be achieved. The complexity to measure the vertical velocity translated in noisy graphs that proved the inability of determining a maximum peak in the cross-correlated signal.

Before the analysis underwent a further step in an attempt to improve the obtained results, the same process was repeated but skipping the even frames instead of taking every consecutive frame. This was thought to be helpful for the analysis in the way that vertical velocity may not vary significantly within two consecutive images that are separated by a small period of time but it may have a higher rate of variation in between more distant time points. In every spatiotemporal analysis of frames there is always an optimum temporal increment which should be large enough in order to describe a significant variation of data but not too large so that the correlation between the data is lost. In our case it should be large enough to show vertical displacement but not smaller than a wavelength so that the vertical displacement vectors belong to the same pedal wave. The analysis proved that the optimum temporal increment was 2 frames. This way, the results improved significantly up to the point that some periodicity could be observed in the

vertical component of the velocity vectors in some of the experiments. However, it was thought that the results could still be improved and a displacement analysis was carried out.

3.3.2 Displacement Analysis

Once proven that the velocity analysis did not entirely yield the desired results, the next approach was to measure displacement instead of velocity. Velocity measures the displacement within two consecutive time points, which for small values may not vary significantly enough to produce proper results. However, if the displacement is measured within every time point in relation to a fixed initial time, the variation will be larger and thus, the possibilities of appreciating wave pattern will be higher.

To measure the vertical displacement, the raw images were cropped into windows of size 96x64. By observing the first image of each experiment, a pixel was selected in order to be the center of the first window. Then, the displacement of the particle in the center of the window was calculated by interpolating its horizontal velocity. The center pixel of the second window (cropped from the second image of the sequence) was the position of the center of the first window plus the displacement of the fluid particle in it. This process was repeated for every image within the same experiment in such way that the net horizontal displacement of the fluid particles in all the cropped windows was nearly zero, but they exhibited vertical displacement.

In the first instance, the PIVlab software was thought to be the most suitable method to perform the velocity field analysis of the particles in the fluid of the cropped windows. However, this idea was soon discarded owing to the impossibility of including PIVlab in a MATLAB routine. PIVlab software only provides the option of entering the input images as bmp/ tiff/ jpeg files, and this would have turned into an unmanageable process due to high number of windows in each experiment. The solution was to make use of a MATLAB code written by Dr. Geno Pawlak (Dept. Mechanical and Aerospace Engineering, University of California San Diego), that performs the same task as PIVlab, achieving similar results. Moreover, this code includes a median filter with the purpose of minimizing the filtering errors along the edges. The code was modified in order to take

the cropped windows as an input. The parameters of the interrogation windows were initially set (both for the course and the fine grid) and each cropped window was evaluated against the initial one.

The output of the software described above yielded the displacement matrices in the vertical axis for each cropped window in relation with the first one. The average of the values of every displacement matrix was computed with the aim of obtaining a vertical mean displacement vector. This vertical displacement was plotted against the number of cropped windows in order to qualitatively observe the obtained pattern. However, the results obtained by this method did not produce consistent graphs that showed no improvement at all with respect to the velocity analysis.

3.3.3   Measuring Algorithms

In order to calculate the pedal wavelength, a MATLAB code was written in such way that the average of the signal was computed and every value higher than the average was considered to belong to the pedal wave, whereas every value lower than the average was considered to be part of the interwave region. This way, by measuring the number of pixels higher than the mean value, an estimation of the pedal wavelength could be obtained.
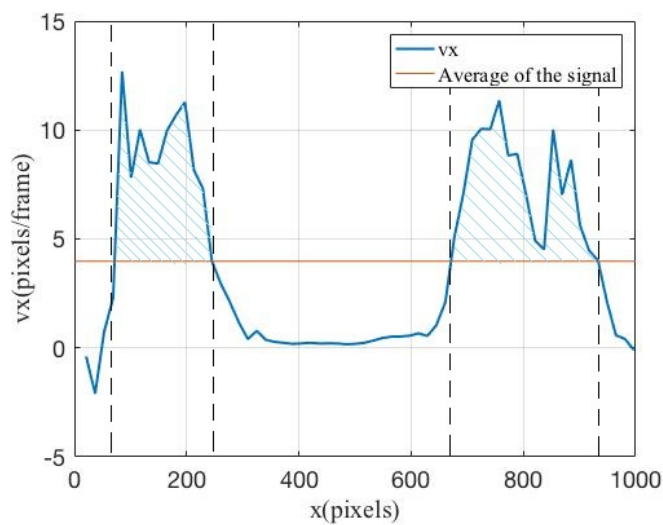
Fig.3.5. *Horizontal velocity vector of the ventral foot of a slug at a certain instant. The striped regions correspond to the areas considered to belong to pedal waves according to the written algorithm.*

Moreover, it is important to highlight that due to the selected interrogation window size in the PIVlab software, each velocity vector provided was in fact 16 pixels away from the previous one. This way, one unit in our correlation graphs will correspond to 16 pixels in our images.

The other measurement we needed to perform was the lag between the horizontal and vertical functions. A good method to compute the delay between two signals is the standard cross-correlation. When cross-correlating one signal with the other, the maximum peak (or the minimum if they are inversely correlated) will correspond to the point where both functions have the best alignment. That is, the maximum/minimum of the cross-correlation function will be located at the value for the lag between the two signals. For our purpose, the MATLAB function "*finddelay*" will be used. This function returns an estimate of the lag between two signals via cross-correlation.

4. RESULTS

The locomotion of a crawling slug or snail is based on a train of pedal waves which produce both horizontal and vertical displacement of the particles in its ventral foot. The first step previous to the realization of the analysis was to validate our method. For this purpose, the results obtained from PIVlab after being filtered; were converted into physical units in order to compare them with values retrieved from other studies. The total crawling speed of gastropods varies among different species, but for leopard slugs, similarly to banana slugs; is usually of the order of 1.5 mm/s. They usually exhibit more that 20 pedal waves which can have a velocity up to 4.5 times greater than the overall crawling speed [5]. The next graph shows the comparison between the magnitudes of both the horizontal (vx) and vertical (vy) components of the instantaneous velocity of the particles of the ventral foot at a time instant when a pedal wave is traversing them. The conversion into physical units has been computed knowing that the pixel size of the images is 67.7 μm x 67.7 μm and the time between two consecutive frames is 1/15s. According to the study "*Mechanics of the adhesive locomotion of terrestrial gastropods*", the results for the magnitude of the speed of pedal waves are consistent with the values obtained from our calculations:
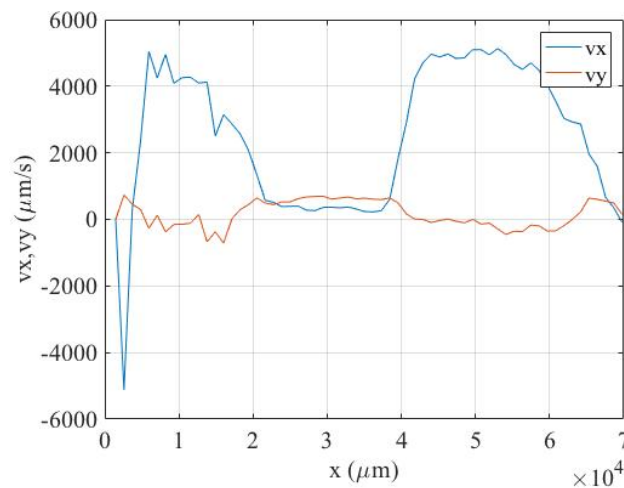
Fig.4.1. *Horizontal (vx) and vertical (vy) components of the instantaneous velocity of the ventral foot of a leopard slug during the passage of a pedal wave. At this specific instant, the horizontal velocity of the pedal wave reaches a maximum value around 5mm/s.*

But rather than measuring the magnitude of the velocity of pedal waves, the main purpose of the analysis was to prove its periodic character. To achieve this goal, the velocity vectors were cross-correlated with themselves in an attempt to observe if the arrangement describing them could be considered a wave. In a circular autocorrelation, there will always be a maximum peak at the point where the lag is zero. Furthermore, provided that the signal under study is periodic, the autocorrelation function should be periodic too, having peaks at the integer multiples of the period. The following graphs show a canonical example of how a wave pattern must look when cross-correlated with itself. The data in these plots has been retrieved from an experiment carried out by an investigation group in Universidad Carlos III de Madrid:
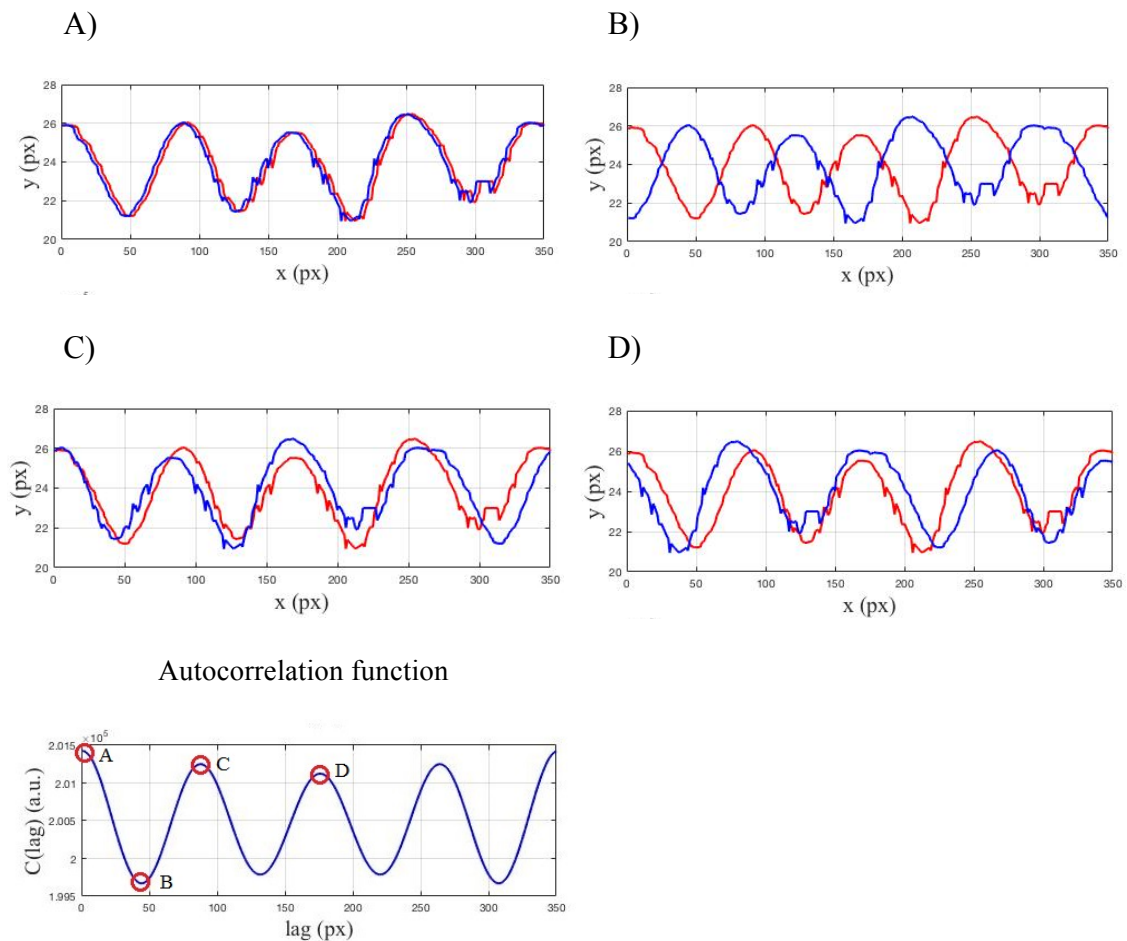
Fig.4.2. Canonical example of the autocorrelation function of an ocean wave. Plots A-D show the correlated function at different stages of the process. The bottom plot contains the autocorrelation function obtained from the previous stages A-D. The maximum peaks indicate a periodicity of 87.5 pixels.

The bottom subplot of Figure 3.2 shows a symmetric graph with clear maximum peaks at multiples of the waves period, proving that the fluid under study is following a wave pattern. When this procedure was repeated with our data, diverse results were obtained.

4.1 EXPERIMENT A

The lapse sequence of the first experiment contained 173 frames. After computing the instantaneous velocity field of each consecutive frame and filtering the velocity vectors by region and modulus, the velocity field of the ventral foot of the gastropod, at the chosen time instant; had the following appearance:
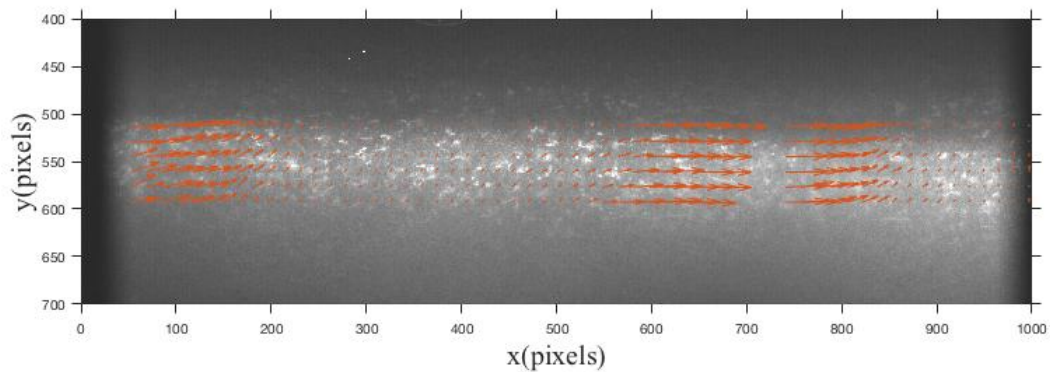
Fig.4.3. *Instantaneous velocity field of the ventral foot of the leopard slug of experiment A. The vectors of higher magnitude belong to regions under a pedal wave whereas the smallest vectors correspond to interwave regions. Two different pedal waves can be observed.*

Then, the analysis continued by auto correlating the filtered horizontal component of the velocity vector with the aim of assessing its periodicity. The following graphs follow the same structure as Fig.3.2 when correlating the horizontal velocity vector with itself:

A)

B)

C)   Autocorrelation function
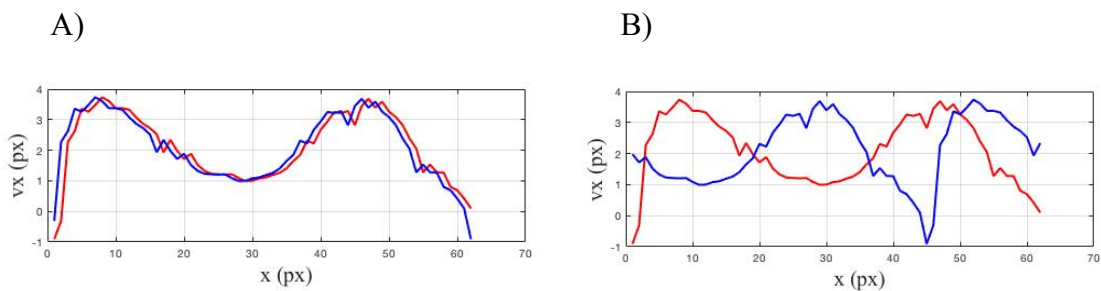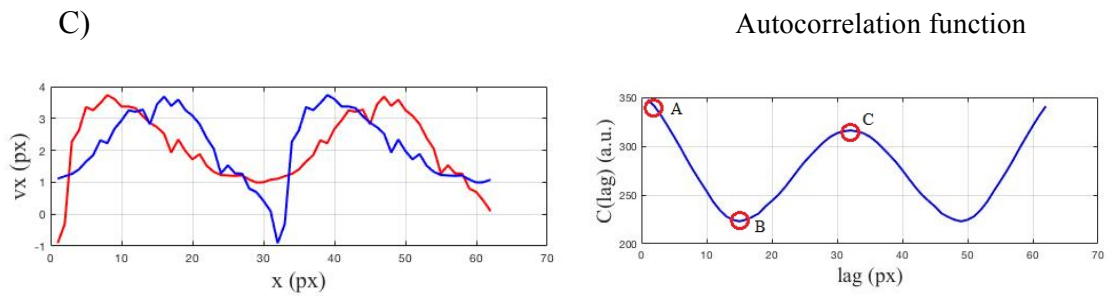
Fig.4.4. Graphs A-C show the averaged horizontal velocity function of the ventral foot of the gastropod in experiment A at different stages of the correlation process. The right bottom subplot represents the autocorrelation function.

A clear maximum can be observed indicating that the horizontal component of the signal of the instantaneous velocity at this time point exhibits a periodicity of **32 pixels.** Due to the size of the interrogation window selected in the PIVlab analysis, each velocity vector provided by this software is 16 pixels away from the previous one. This means that one pixel in our graphs correspond to 16 pixels of the images. This way, our signal will have a period of **512 pixels**. The algorithm explained before in section 3.2 was implemented in order to calculate the pedal wavelength of the horizontal component (λ_x). The instant taken in this first experiment shows two pedal waves in the same frame. For this reason, λ_x will be the average of the wavelength of the two pedal waves. However, in this case both wavelengths shown in the previous figure had a value of **15 pixels** in the correlation graphs which equals to **330 pixels** in the images.

The same process was repeated with the vertical component of the velocity vectors. The vertical component in this experiment has an average value approximately 4 times smaller than the horizontal component. For this reason, the results obtained were not as conclusive as for the horizontal axis:

A)

B)

C)

Autocorrelation function
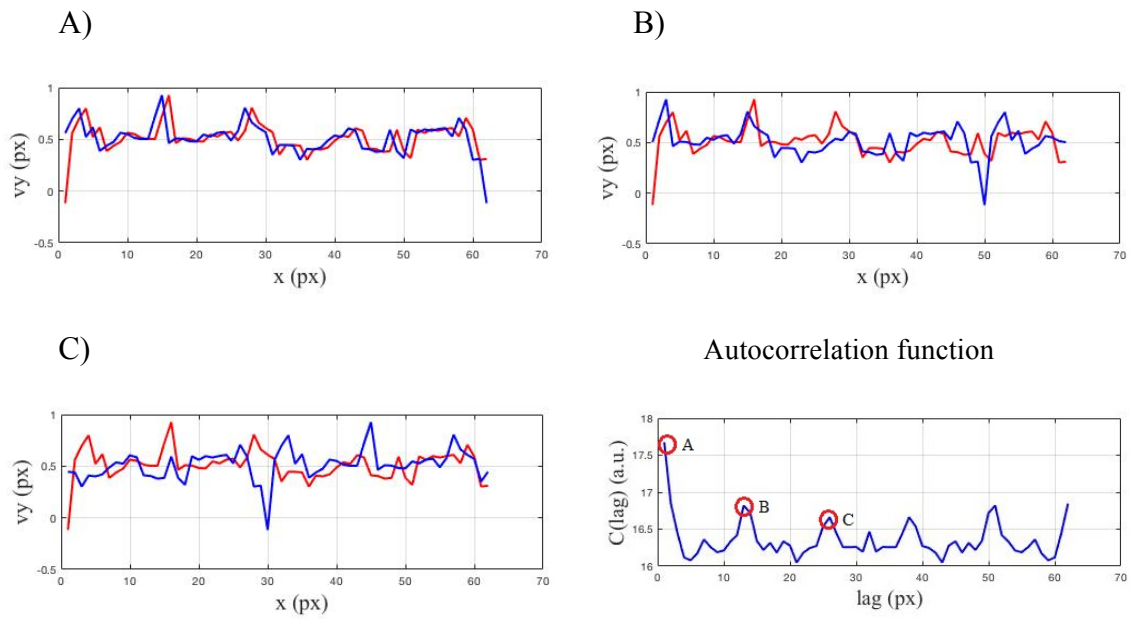
Fig.4.5. Graphs A-C show the averaged vertical velocity function of the ventral foot of the gastropod in experiment A at different stages of the correlation process. The right bottom subplot represents the auto correlation function.

Since the vertical autocorrelation did not yield clear maximums and the wavelength of the signal could not be computed; the procedure was repeated doubling the temporal increment of frames. This improved the results but, still the graphs did not allow the calculation of the vertical pedal wavelength (λ_y).

A)

B)

Autocorrelation function
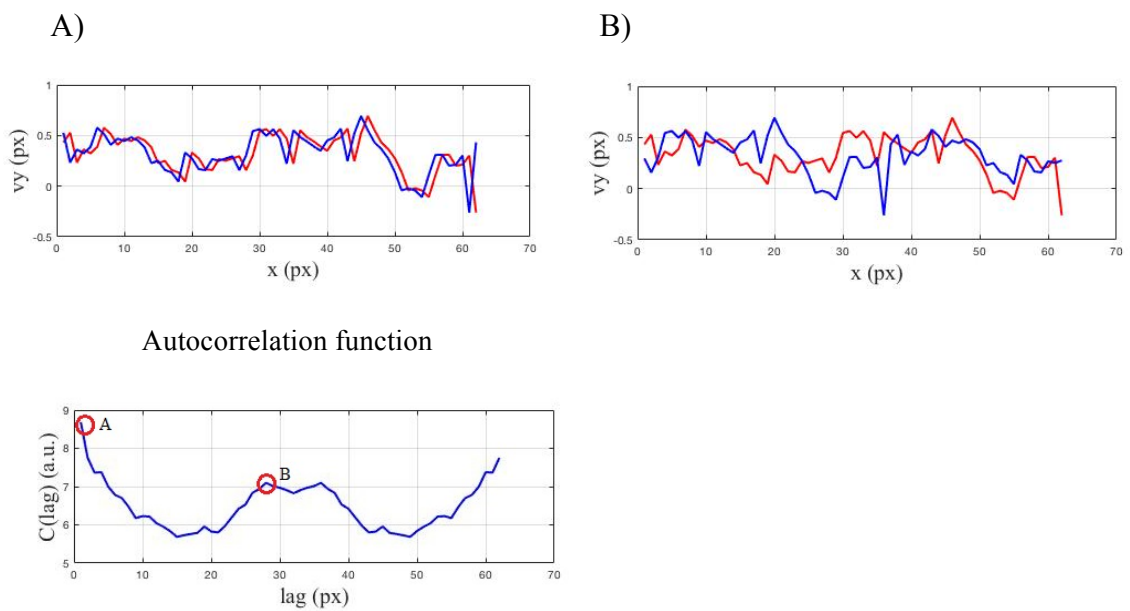
Fig. 4.6. Graphs A-B belong to stages of the auto correlation procedure of the averaged vertical component of the velocity when computed with a double temporal increment. The bottom plot shows the auto correlation function

Even if the results improved when using a larger temporal increment, the wave pattern of the vertical component could not yet be detected. The last attempt to characterize the vertical velocity was to perform a displacement analysis. This time the analysis was not accomplished with PIVlab but with several MATLAB codes. However, these codes do not include many of the options that PIVlab does, such as vector validation or multigrid correlation. For this reason, the results obtained when auto correlating the vertical displacement function were not consistent enough and did not introduce new improvements with respect to the velocity analysis:
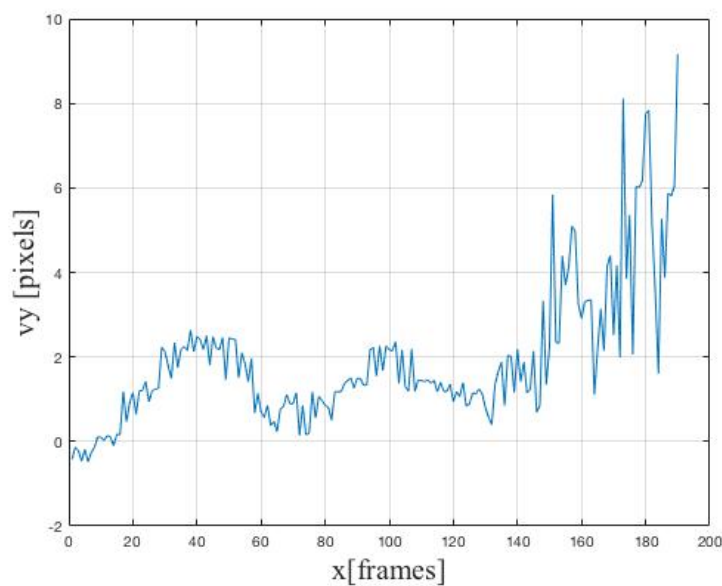
Fig.4.7. Averaged vertical component of the displacement of the ventral foot of the leopard slug in experiment A during the whole lapse sequence.

As it can be noticed in Fig.4.6, the displacement method provided quivering graphs which led to measurements with high amounts of noise that were not conclusive in order to validate our model. Moreover, the displacement analysis was not consistent through all the experiments. For these aforementioned reasons, the results obtained from the displacement analysis were not taken into account in any of the trials, and will not be presented in further experiments. Thus, it was not possible to calculate a value for the pedal wavelength (λ) and a value for the lag between the horizontal and vertical displacement functions in experiment A.

4.2 EXPERIMENT B

The sequence of images for this experiment contained 193 frames. The workflow of the velocity analysis was repeated for this second experiment. In the time instant selected, the following velocity field could be observed:
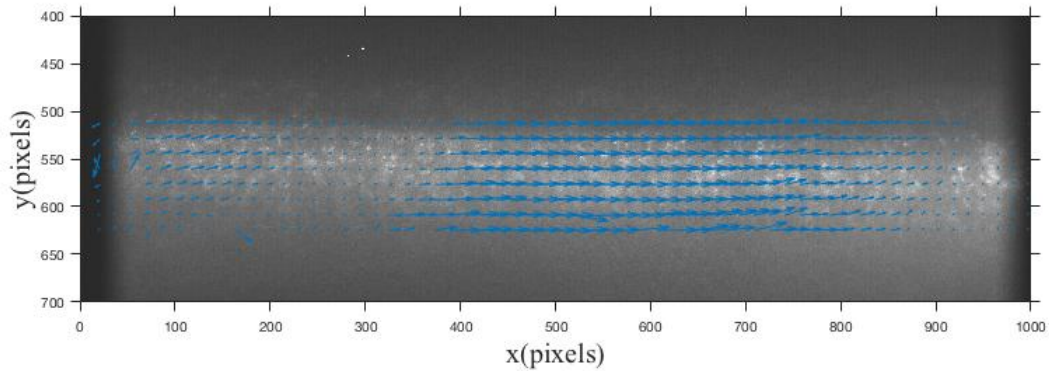
Fig. 4.8. *Instantaneous velocity field of the ventral foot of the leopard slug of experiment B. The vectors of higher magnitude belong to regions under a pedal wave whereas the smallest vectors correspond to interwave regions. One complete pedal wave can be observed.*

In this prior figure, only one complete pedal wave and half of the next one can be appreciated. Optimum experiments should include the maximum number of pedal waves in the same frame as possible, so that the periodic character of the signal can be well accepted. However, the analysis was limited in this sense, since the raw images that were evaluated included a maximum number of two pedal waves per frame.

The cross-correlation of the horizontal component of velocity provided a wave pattern easy to see:

A)

B)

C)   Auto correlation function
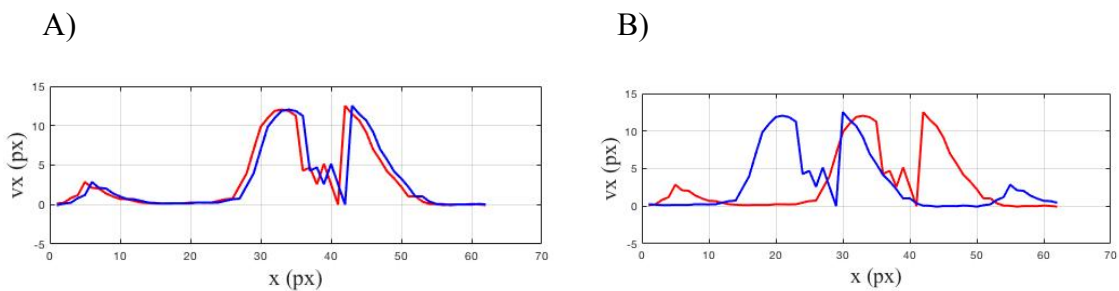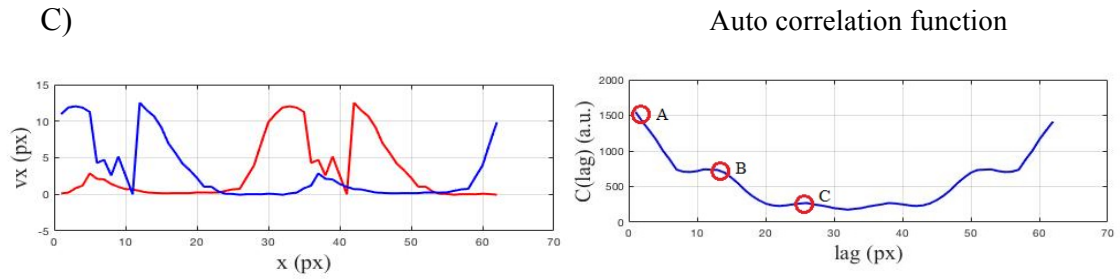
Fig.4.9. Graphs A-C show the averaged horizontal velocity function of the ventral foot of the gastropod in experiment B at different stages of the correlation process. The right bottom subplot represents the auto correlation function.

Consistent with the results in experiment A, the periodicity of the signal was **32 pixels** in the graph, that again corresponds to a real value of **512 pixels.** Moreover, the computed pedal wavelength (λ_x) of this second animal was **19 pixels,** that is λ_x equals **304 pixels** for experiment B. When repeating the same procedure for the vertical axis, the results were not the desired ones since no pedal waves could be appreciated at all. In order to avoid repetition, the next results displayed will be the ones for the double temporal increment:

A)   B)

C)   Auto correlation function
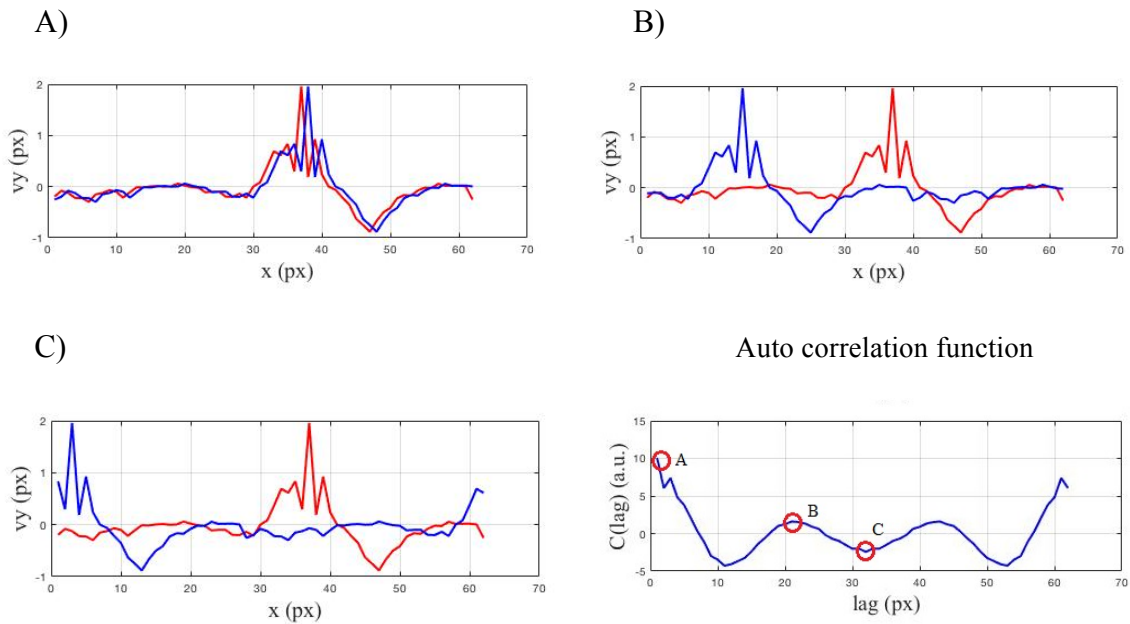
Fig.4.10. Graphs A-C belong to stages of the auto correlation procedure of the averaged vertical component of the velocity when computed with a double temporal increment. The right bottom plot shows the auto correlation function.

The computed pedal wavelength for the vertical component of velocity (λ_y) from the graphs was **15 pixels,** which translates into **240 pixels** in the images. However, the pedal wavelength must be equal for both the horizontal and vertical functions. For our purpose,

we will compute the arithmetic mean in order to draw the point in our model. This way, the taken value for the wavelength (λ) for this experiment will be **272 pixels**. In order to plot the values for the pedal wavelength and the lag, both values need to be dimensionless. To achieve this, the values have been normalized by the wavelength of the train of pedal waves (L), that has been computed using the same algorithm as for the pedal wavelength.

$$\lambda_{adim} = \frac{\lambda(pixels)}{L(pixels)} \qquad [26]$$

$$l_{adim} = \frac{l(pixels)}{L(pixels)} \qquad [27]$$

For experiment B, the value of L was **352 pixels**, so the dimensionless value of the pedal wavelength, λ_{adim} yielded **0.7727**. Once the periodicity of the waves had been proven, the next step was to calculate the lag between both the horizontal and vertical waves. This was achieved by plotting both waves for the same time instant (frame):
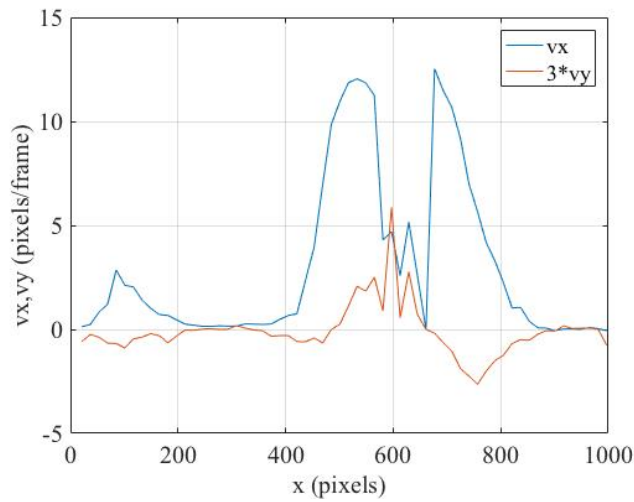
Fig.4.11. *Horizontal (vx) and vertical (vy) averaged components of the instantaneous velocity of the ventral foot of the leopard slug in experiment B, during the passage of a pedal wave. Notice that the vertical component has been multiplied by 3 for visualization purposes.*

The MATLAB function "finddelay" yielded a result of **240 pixels** for the delay between the horizontal and vertical pedal waves. Again, normalizing this value by the wavelength of the train of waves, L; the dimensionless value for the lag of experiment B is **0.6818.**

4.3 EXPERIMENT C

The raw data of experiment C consisted of 198 images. The PIVlab analysis yielded the instantaneous velocity field for every pair of consecutive frames. After filtering the vectors, the following instant was selected to perform the further analysis of experiment C:
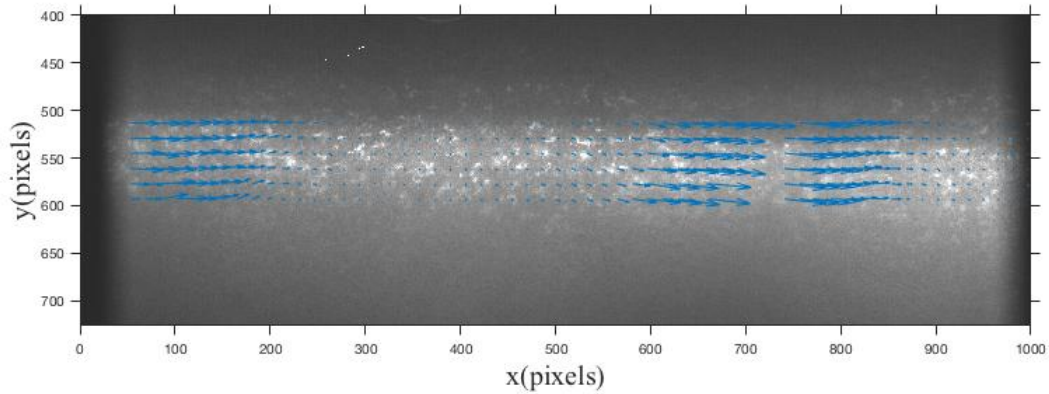
Fig.4.12. *Instantaneous velocity field of the ventral foot of the leopard slug of experiment C. The vectors of higher magnitude belong to regions under a pedal wave whereas the smallest vectors correspond to interwave regions. Almost two complete pedal waves can be observed.*

In the instant selected, almost two complete pedal waves can be appreciated and thus, this will provide better results for the periodicity of the waves. The velocity analysis started by checking the periodic character of the horizontal component of the velocity of the pedal wave:

A)

B)

40

C)   Autocorrelation function
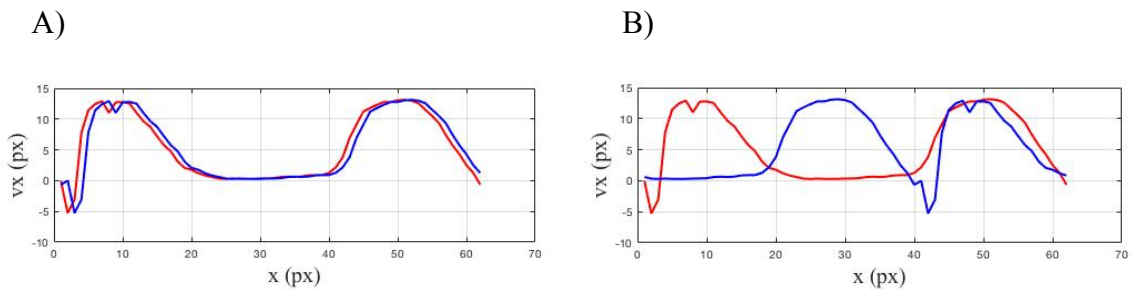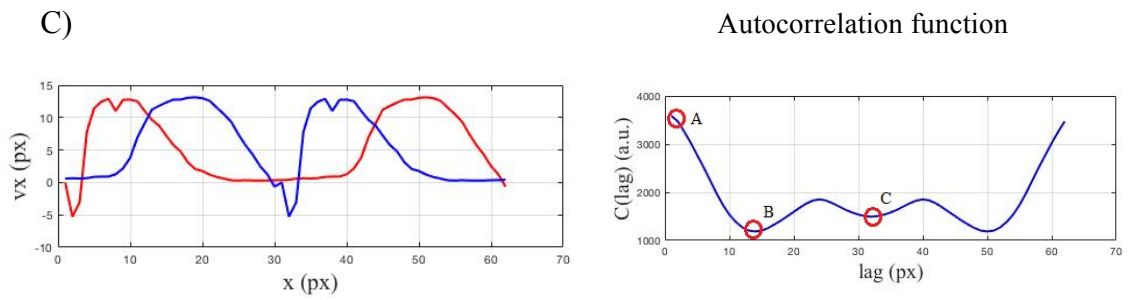
Fig.4.13. Graphs A-C show the averaged horizontal velocity function of the ventral foot of the gastropod in experiment C at different stages of the correlation process. The right bottom subplot represents the auto correlation function.

For this slug, the horizontal velocity yielded a periodicity of **32 pixels,** that is in the real frame **512 pixels.** The horizontal pedal wavelength (λ_x) was computed by making the average between the pedal wavelength of both pedal waves giving rise to a value of **240 pixels.**

The next step was to repeat the procedure for the vertical velocity. However, performing the PIVlab analysis with every frame did not produce optimum results. When the analysis was redone doubling the temporal increment, that is, skipping the even frames of the lapse sequence of images; the following results were obtained for the vertical component of velocity:

A)   B)

C)   Auto correlation function
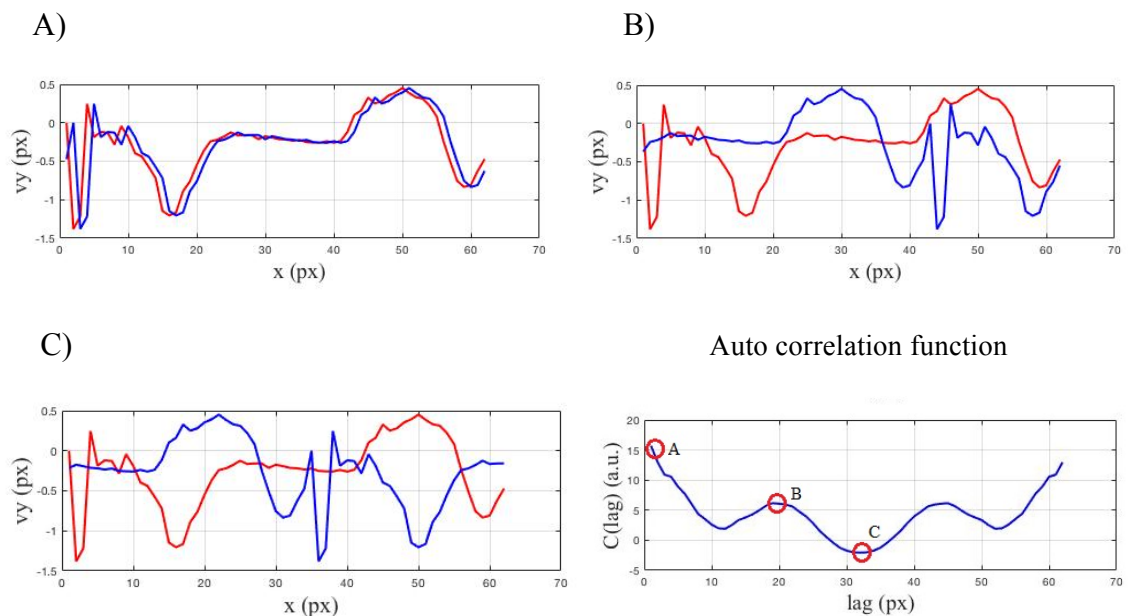
Fig. 4.14. Graphs A-C belong to stages of the auto correlation procedure of the averaged vertical component of the velocity when computed with a double temporal increment. The right bottom plot shows the auto correlation function.

For experiment C, the computed vertical pedal wavelength (λ_y) was again **240 pixels**; a consistent value with the horizontal pedal wavelength (λ_x). Thus, the average pedal wavelength (λ) of this experiment was considered to be **240 pixels**. Again, in order to make this parameter dimensionless; it was normalized by the wavelength of the train of waves, L. L was computed by counting the number of pixels that had a value lower than the average of the signal, yielding a value of **400 pixels**. Thus, the dimensionless value for the pedal wavelength, λ_{adim} was **0.6000**.

The final step was to compute the lag between both the vertical and horizontal velocity functions. The following plot shows both components for the same time instant:
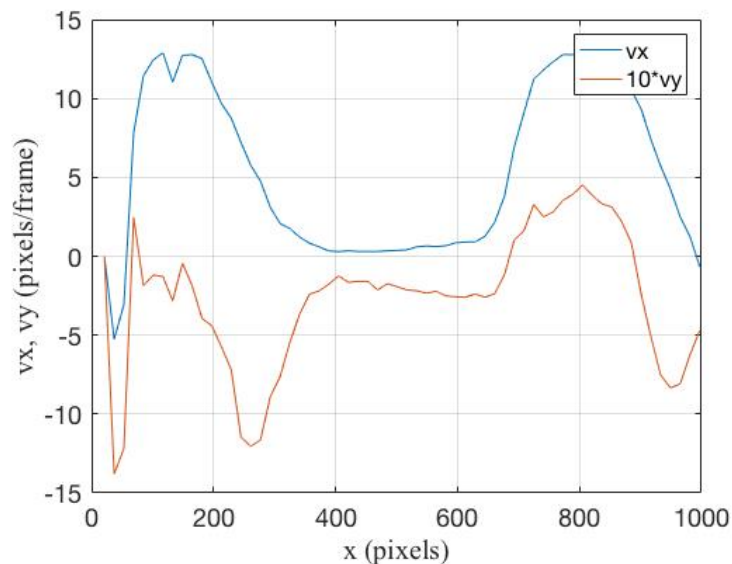
Fig.4.15. *Horizontal (vx) and vertical (vy) averaged components of the instantaneous velocity of the ventral foot of the leopard slug in experiment C, during the passage of a pedal wave. Notice that the vertical component has been multiplied by 10 for visualization purposes.*

Making use of the MATLAB function "finddelay", the lag between the two component signals was **192 pixels.** The same way the pedal wavelength (λ) was normalized, the dimensionless value of the lag between the horizontal and vertical functions, $l_{adim,}$ was **0.4800.**

4.4 EXPERIMENT D

The last experiment that will be presented in this thesis included 181 images. The velocity field for the selected time instant is shown in the figure below:
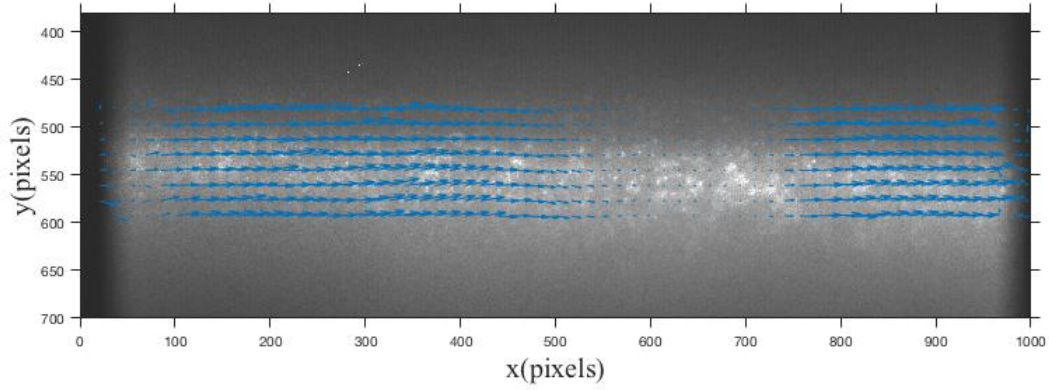
Fig.4.16. *Instantaneous velocity field of the ventral foot of the leopard slug of experiment D. The vectors of higher magnitude belong to regions under a pedal wave whereas the smallest vectors correspond to interwave regions. Almost two complete pedal waves can be observed.*

Proceeding as in the previous three experiments, the horizontal component of the velocity was cross correlated with itself, providing the following results:

A)

B)

C)

Auto correlation function
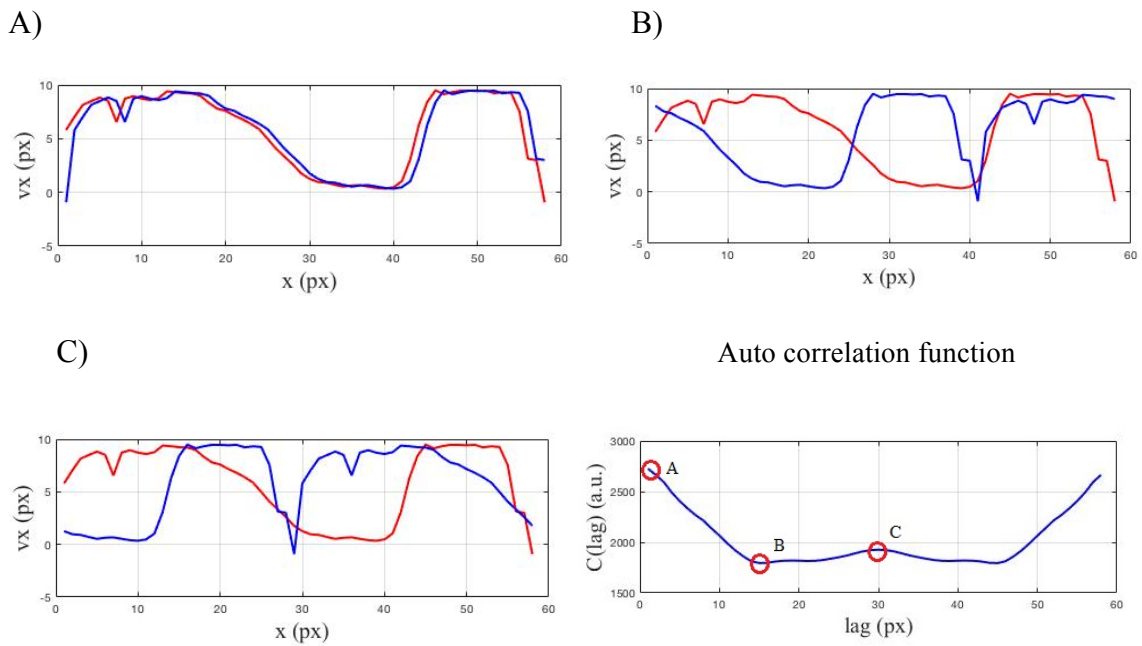
Fig.4.17. *Graphs A-C show the averaged horizontal velocity function of the ventral foot of the gastropod in experiment C at different stages of the correlation process. The right bottom subplot represents the auto correlation function.*

To proceed, the values of the two horizontal pedal wavelengths (λ_x) were computed and averaged yielding a result of **272 pixels.** Moreover, consistent with previous experiments, the periodicity showed a value of **30 pixels** in the graphs, **480 pixels** in the images.

The same process was done but this time with the vertical component of the velocity field. Since it has been experimentally proven that the optimum time increment for the analysis is 2 frames the graphs below show the steps of the cross-correlation process for the vertical velocity of the ventral foot when the PIVlab analysis was performed just taking the odd frames:

A)

B)

C)

Auto correlation function
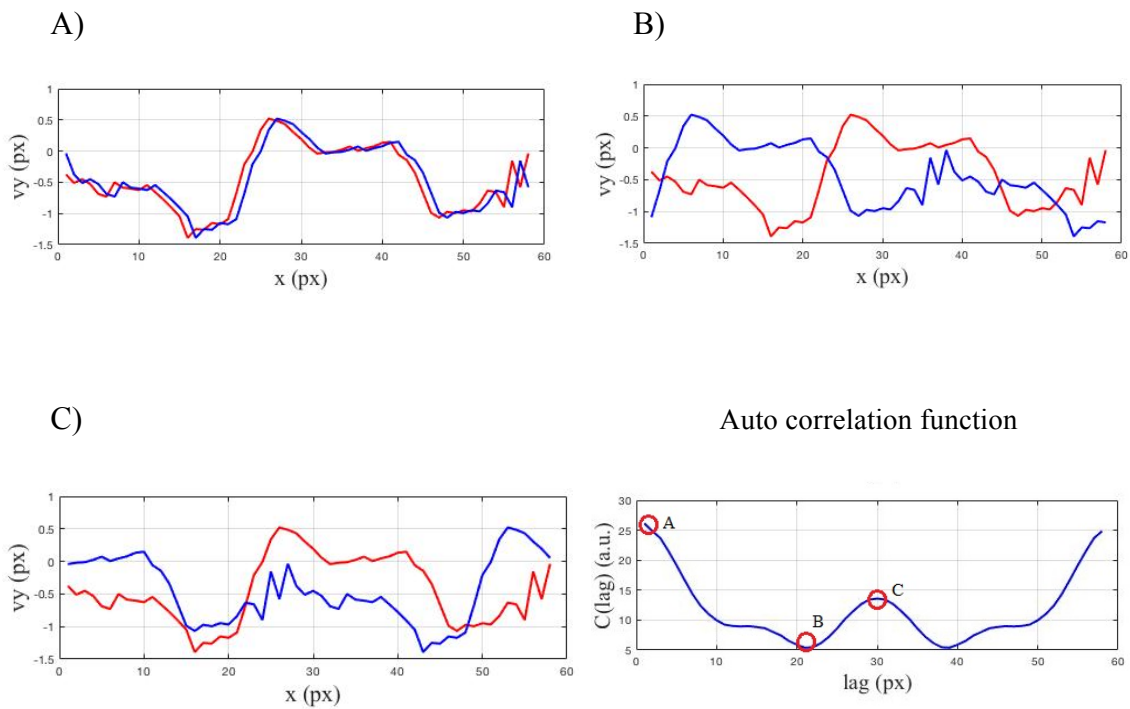
Fig. 4.18. Graphs A-C belong to stages of the auto correlation procedure of the averaged vertical component of the velocity when computed with a double temporal increment. The right bottom plot shows the auto correlation function.

Again, the vertical pedal wavelength (λ_y) was computed providing a result of **304 pixels**. This way by averaging the values of the pedal wavelength for both the horizontal and vertical components, λ took a value of **288 pixels.** To normalize the results, the wavelength of the train of waves, L was computed giving a result of **320 pixels.** This way the value of λ_{adim} of experiment D was set to **0.9000.**

Finally, the lag between the horizontal and vertical waves was computed by plotting these functions for the same time instant in the following graph:
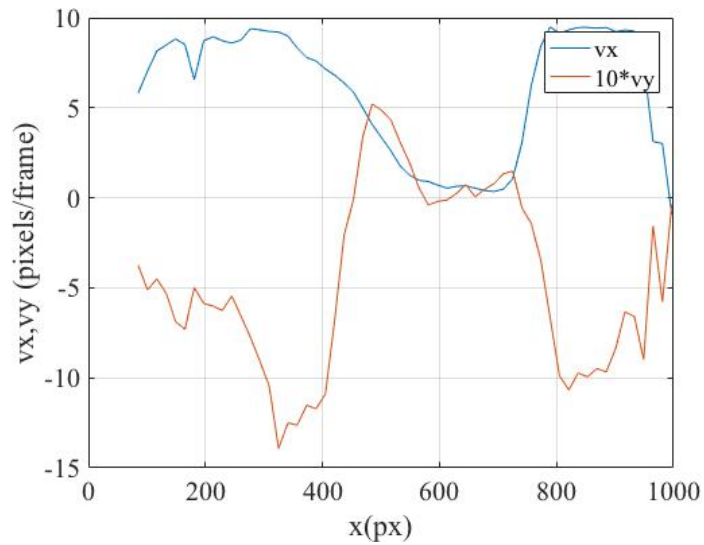
Fig.4.19. Horizontal (vx) and vertical (vy) averaged components of the instantaneous velocity of the ventral foot of the leopard slug in experiment D, during the passage of a pedal wave. Notice that the vertical component has been multiplied by 10 for visualization purposes.

The obtained result for the lag was **240 pixels.** By normalizing the lag by the wavelength of the train of waves, the obtained result for l_{adim} was **0.7500.**

5. DISCUSSION

Before developing the analysis in this thesis, it was believed that the experiments carried out in 2010 will not produce any significant results for the vertical component of the pedal waves. The magnitude of the displacement in the axis perpendicular to the motion direction of the animal, had been proven to be very small (of the order of 70 μm) in previous studies [5]. The main concern prior to the analysis was that any variation in the vertical axis could be smaller than the size of the pixels in our images (67.7 μm). Still, the analysis was carried out hoping that the Particle Image Velocimetry technique could improve the results obtained previously through the measurement of the gray levels of the pixels in images of the ventral foot of terrestrial gastropods. For this reasons among others, the fact of being able to measure this velocity in three different time instants corresponding to three different experiments is already something that can be considered significant.

Prior to any discussion of the results, they will be summarized in the following table:

TABLE 5.1.

RESULTS OBATINED FOR THE WAVELENGTH, PEDAL WAVELENGTH AND LAG OF THE 4 EXPERIMENTS ANALYZED

	L (pixels)	λ_x (pixels)	λ_y (pixels)	λ (pixels)	λ_{adim}	l (pixels)	l_{adim}
Experiment A	-	330	-	-	-	-	-
Experiment B	352	304	240	272	**0.7727**	240	**0.6818**
Experiment C	400	240	240	240	**0.6000**	192	**0.4800**
Experiment D	320	272	304	288	**0.9000**	240	**0.7500**

The next step in order to assess the results obtained is to plot the values for the dimensionless pedal wavelength and lag in the graph in Fig.2.3. The dark regions in this graph show the possible values for the pedal wavelength and lag that allow locomotion to happen independently of the rheological properties of the mucus. Thus, by plotting the results obtained experimentally, an insight about the validity of the model can be acquired:
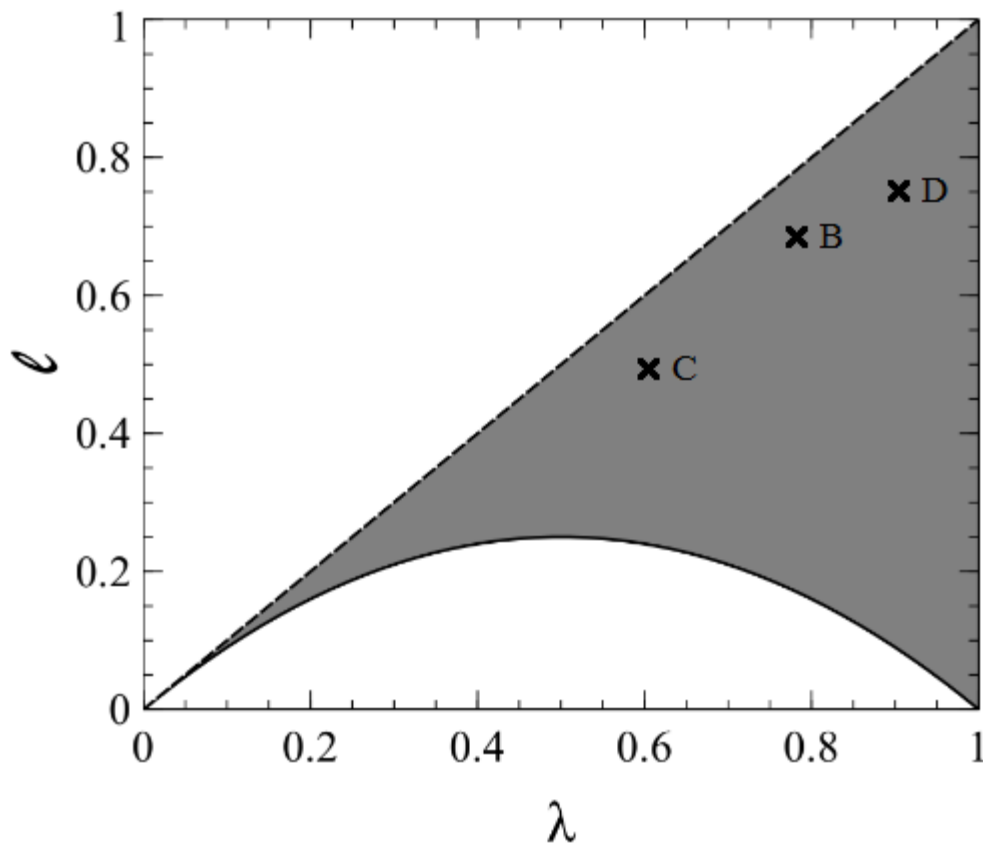
Fig.5.1. Display of the results of the analysis for experiments A-D on the allowed regions where locomotion is possible according to the proposed theoretical model.

In the previous graph, it can be seen how three out of the four experiments analyzed yielded results that fit in the region proposed in the theoretical model. However, the model cannot be validated and generalized just based on four selected time instants, specially taking into account that in every time instant selected, the vertical pedal waves could be appreciated. The obtained results should be systematic for every instant of each experiment, but there were many moments where the pedal waves in the vertical axis could be observed.

47

This way, even if many time instants did not allow the measurement of the vertical pedal wave, the ones in which it could actually be observed, provided values that fit in the proposed regions. This implies, that even if the analysis could not be entirely accomplished, the results are consistent with the hypothesis put forward in the theoretical model.

It is quite complex to compare our results with other previous studies, since there are no other investigations on adhesive locomotion of leopard slugs. However, there is some physical parameters of garden snails that can be extrapolated to our slugs. Adult garden snails have an average length of 5-7 cm and their pedal wavelength varies in a range of 2-5.5 mm [5]. On the other hand, the ventral foot of adult leopard slugs has a length of 10-20 cm. The results obtained in our analysis concluded that the pedal wavelength of leopard slugs ranges between 21-26 mm. These values are consistent with the ones of gardens snails taking into account that leopard slugs are of the order of 4 times larger than garden snails.

Even if it is not possible to assure that adhesive locomotion of leopard slugs follows the proposed model, the fact that 75% of the trials analyzed produced validating results, proves that there are high possibilities of adhesive locomotion to happen without a non-Newtonian mucus. However, not every time instant of the experiment produced the desired results, and this is, among other reasons, due to the several limitations that this analysis had to face.

5.1 LIMITATIONS OF THE ANALYSIS

The first limitation relevant to be mentioned is the old nature of the images. The experiments were carried out in 2010 with a slow-motion camera of 1024x1024 pixels resolution (1.05 Megapixels), which produced images with pixel size of 67.7 um. The pixel size is in many instants bigger than the variation of the vertical component of the velocity of the pedal wave. This is why the study "*Mechanics of adhesive locomotion of terrestrial gastropods*" developed in 2010, could only compute the magnitude of the vertical displacement of the foot of the gastropods under study but not its variation. At

first the experiments were performed with garden snails and the magnitude of the vertical displacement of their ventral foot was computed by means of measurements of the grey-levels in the images. However, the variation of the vertical component of the velocity of the ventral foot of gastropods could not be quantized. This limitation pushed the research team to repeat the experiments with leopard slugs, taking advantage of the bright spots present in their bodies as tracer particles for the Particle Image Velocimetry analysis.

Another limitation that this analysis faced is the common limitation in Particle Image Velocimetry procedures: the selection of an optimum temporal increment. In our case, the vertical component of the velocity of the pedal waves varies less than a pixel in two consecutive frames. This implies that a small temporal increment will not allow the measurement of parameter that slightly change over time. Opposed to this, the selection of a temporal increment too high, will make the results lose correlation. If the analysis is performed between two frames which are very separated in time compared to the period of the pedal waves, the obtained measurements will belong to two different pedal waves and thus the results will be incorrect. Taking this into account, the encountered optimum time increment was 2 frames. With this temporal increment, the variations in the vertical axis could be evaluated and it was ensured that the results belonged to the same pedal wave.

Moreover, Particle Image Velocimetry analysis need to deal with unexpected events such as the out-of-pattern motions and the loss of the tracer particles from the illuminated plane due to the three-dimensional nature of the fluid under study. These two limitations are the major sources of error in every Particle Image Velocimetry analysis.

The next limitation encountered was related to the nature of the experiments which provided the raw images for this thesis. In order to measure the periodic nature of any signal it is convenient to have the maximum number of periods as possible. However, the images taken in these experiments included a maximum number of two pedal waves. During the performance of the experiments, the images were focused on a small area of the ventral foot in order to maximize the pixel resolution. Thus, when auto correlating

both the horizontal and vertical velocity functions, only one (or two at maximum) period could be measured.

5.2 FURTHER RESEARCH

The presented work is just the first attempt to measure the variation of vertical velocity of pedal waves in terrestrial gastropods. Before accomplishing the analysis, the expectations about being able to get proper measurements were not high. The small magnitude of the vertical component of velocity together with the complexity of measuring it from images of not enough quality, were the main reasons why this project was discarded in 2010. But despite all these complications, the analysis needed to be finished even if the obtained results were not conclusive.

Surprisingly, some measurements could be obtained for the variation of the vertical velocity of the particles in leopard slug's ventral foots. The positive output of this project encourages the continuation of the analysis of adhesive locomotion of terrestrial gastropod knowing the many potential applications it can have in the biomimetic robotic field.

In order to improve the results presented in this thesis, some guidelines should be followed. These procedures should start by repeating the experiments, this time using cameras of higher resolution and lower pixel size. Huge advances have been made since 2010 regarding digital cameras. The reduction of the pixel size would be critical if repeating this analysis since the variation in the vertical axis would yield clear wave patterns simple to evaluate. Furthermore, this new set of experiments should image the complete ventral foot of the gastropod, allowing the observation and measurement of several pedal waves. More modern cameras have better resolution so there is no more need to focus the images on a small area of the animal's ventral foot.

Moreover, the results could be improved by playing with the parameters of the PIV analysis. The smaller the interrogation window size is, the higher amount of velocity vectors will be obtained in the instantaneous velocity field. However, there is a trade-off

between the amount of data obtained and the computational cost of the analysis. For these reasons, even if the selected window size in this thesis yielded some functions were the pedal waves could be appreciated and measured, the selection of a smaller window will produce less noisy signals and better results.

6. ECONOMIC ENVIRONMENT

The purpose of this section is to break down the total budget that made possible the realization of this project and to evaluate the possible future economic impact that the applications derived from it can cause.

6.1 FINANCES

The analysis performed in this thesis would not have possible without the set of experiments carried out in 2010 in California (US) by Janice H. Lai, Juan C. del Alamo, Javier Rodríguez Rodríguez and Juan C. Lasheras. The main costs of these experiments were the laser, the camera and the slugs themselves. It is relevant to highlight that in order to determine their final cost, it is necessary to take into account the amortization time of the lab equipment (laser and camera) which is usually stipulated to be 60 months. This way, the budget included in the following table regarding the laser and camera must be calculated knowing that the experiment lasted for 2 months.

TABLE 6.1.

TOTAL COST OF THE SET OF EXPERIMENTS THAT PROVIDED THE RAW DATA FOR THIS THESIS.

	Price per unit	Number of units	Amortization time	Use time	Total
Laser	12,000€	1	60 months	2 months	400€
Camera	50.000€	1	60 months	2 months	1700€
Slugs	30€	10	-	-	300€
					2,400€

Moreover, it is necessary to include the costs of human resources and software that have been necessary to assume during the development of this thesis. These include the hours devoted by a senior engineering to the cause and the cost of a Mathworks[®] license:

TABLE 6.2.

TOTAL COST OF PERSONNEL AND SOFTWARE NEEDED TO COMPLETE THIS THESIS.

	Cost	Time	Total
Senior engineering	60€/hour	15 hours	900€
Mathworks license	450€/year	3 months	115€
			1,015€

This yields a total of 3,415€ as the final budget needed to perform this work.

6.2 ECONOMIC IMPACT

As the work carried out in this project is entirely theoretical, it is complex to assess its economic repercussion straightforward. For this reason, what this section will try to evaluate is the possible financial impact of the biomedical applications it can have. The main focus will be set on the prototype of endoscope developed by Tohoku University (Japan) since it is the most feasible application up to the date.

It is estimated that the annual cost of an endoscopy room in Spain raises up to 349,617.69€. Of this total amount, 65.5% is represented by staffing costs from which 56.3% are direct costs [25]. This value was determined taking into account the cost per year of human resources, equipment, maintenance and the general costs that the hospital assumes during the hours of work of the endoscopy department. Moreover, it is stablished that a gastroscopy procedure has a value of 27.52€ for the public Spanish healthcare system whereas anoscopy has a cost of 15.08€ and colonoscopy of 74.28€ [25].

Furthermore, studies state that the use of endoscopy will grow around 7% yearly until 2021. This growth is own to the generalization of the endoscopy as both diagnostic and interventionist procedures due to its proven efficiency. This way, the global endoscopy market will increase its value up to 1,871 million euros according to the numbers predicted for 2021, reaching a constant yearly growth rate of 6.9% [26].

The opportunity of developing an endoscope based on gastropod's crawling makes it possible to target the damaged area of the gastrointestinal tract straightforward. This leads to a shorter duration of diagnostic endoscopy routines and an increase of the efficiency

during interventionist procedures. Even if it is complex to stablish a number for the economic impact it will have on Spanish healthcare, what it is certain is that in a world where digestive diseases increase yearly; more precise endoscopes will help to save both capital and human resources in endoscopy procedures carried out daily.

7. REGULATORY FRAMEWORK

The set of experiments carried out in 2010 in California (USA), that provides the backbone data for this thesis, involved dealing with gastropods, more in particular with leopard slugs (*Limax Maximus*). The US legislation interprets the term "laboratory animal" as any vertebrate animal produced for or used in research, testing or teaching [20]. Thus, legislation makes a clear division between vertebrates and invertebrates regarding experimenting with them. This is based on the fact that invertebrates (except cephalopods) have much simpler nervous systems than vertebrates, and are formed uniquely by several ganglia interconnected by nerves. Under the Animal Welfare Act (18 December 2007), experiments involving cephalopods are notifiable, but experiments involving the rest of invertebrates do not require any declaration [21].

The main limitations of these experiments were thus, regarding the slugs acquisition and transportation. The United States Department of Agriculture (USDA) states that plant pest permits are needed for the importation of slugs from one state to another. These permits are commonly granted for research and educational purposes. However, to avoid bureaucratic issues; the slugs were purchased in California, the same state where the latter experiments were to be carried out. Moreover, the USDA warns about the danger of live slugs being released into an environment different from their original one, in the purpose of avoiding possible pests or interference with other species [22].

All the experiments were performed under the knowledge of the legislation and in all of them regulations were obeyed and respected.

8. PROJECT SCHEDULING

This project started on February 2018 and concluded on September of the same year. It started with a phase of documentation that lasted around one month and required reading and understanding some papers related to the issue which was to be addressed in this thesis.

Then, several meetings with Javier Rodríguez Rodríguez were needed in order to stablish the scope of the project, solve some doubts about the read papers and work on the proposed model. Once the mathematical model was finished, the analysis of the images started. This stage was the longest in time since it involved getting familiarized with the new software (PIVlab) and writing an own software in MATLAB. Moreover, the fact that the results obtained at first were not as expected made the analysis phase to last until mid-September.

At the same time that the analysis was being carried out, the writing of the present thesis started. However, it was not until the analysis was finished that all the results were evaluated and explained in detail. All these steps were closely monitored by my tutor in order to avoid possible mistakes that would have delayed the end of the project.

9. CONCLUSION

Adhesive locomotion of terrestrial gastropods is of great concern in the biomimetic field for those who try to reproduce it in soft robots capable of performing tasks that rigid robots fail to. It was one century ago when the first studies about the matter were published, solving several questions and formulating new ones. Since then, the study of adhesive locomotion has tried to clarify controversial hypothesis up to the date when the complete mechanism still remains unclear.

The analysis carried out in this thesis tried to give one more turn to the process underlying terrestrial gastropod's locomotion. In the aim to adapt biological processes to the needs of human beings through technology, the theoretical model put forward in this project provides the possibility of reproducing gastropods' motion in a simpler manner. Newtonian fluids are easier to model and easier to be introduced in biomimetic robots, so the possibilities of using them as substitutes for the non-Newtonian slug's mucus opens new lines of investigation in the field.

Provided the initial uncertainty about being able to measure vertical displacement of the ventral foot of leopard slugs, Particle Image Velocimetry technique proved to be an adequate method to study the behavior and variation of the train of pedal waves. The variation of position of the particles in the ventral foot was at some time points greater than the pixel size of the raw images. This, even if still complex, allowed the characterization of the motion of the fluid particles of the body of the leopard slugs under study. This way, even if the vertical displacement could not be appreciated in the experimental images at several time instants, in three out of the four experiments the vertical component could be measured and quantized. The small magnitude of the variation in the vertical axis in comparison with the horizontal one, proves the success of the analysis even if not every time instant could be evaluated.

When comparing the experimental results with the theoretical hypothesis, the three valid measurements obtained were consistent with the model. For this reason, even if it is still

not feasible to generalize the hypothesis for every gastropod species, the results motivate to continue with this research line.

Thanks to the analysis performed, we are closer to the development of biomimetic robots capable of reproducing slugs' adhesive locomotion by means of a Newtonian mucus. The entire potential of adhesive locomotion in the biomedical engineering field cannot still be foreseen, however, it is easy to believe that biological mechanisms developed by nature could appear to be appropriate methods to explore the inner human body and help to produce more accurate diagnoses.

10. BIBLIOGRAPHY

[1] **Chan, B., Balmforth, N. and Hosoi, A.** (2005). "Building a better snail: Lubrication and adhesive locomotion". *Physics of Fluids*, vol. 17, no. 11, p. 113101, 2005.

[2] **P. De Groen**, "History of the Endoscope [Scanning Our Past]", *Proceedings of the IEEE*, vol. 105, no. 10, pp. 1987-1995, 2017.

[3] **D. Hosokawa, T. Ishikawa, H. Morikawa, Y. Imai and T. Yamaguchi**, "Development of a biologically inspired locomotion system for a capsule endoscope", *The International Journal of Medical Robotics and Computer Assisted Surgery*, vol. 5, no. 4, pp. 471-478, 2009.

[4] B**. Chan, S. Ji, C. Koveal and A. Hosoi**, "Mechanical Devices for Snail-like Locomotion", *Journal of Intelligent Material Systems and Structures*, vol. 18, no. 2, pp. 111-116, 2006.

[5] **J. Lai, J. del Alamo, J. Rodriguez-Rodriguez and J. Lasheras**, "The mechanics of the adhesive locomotion of terrestrial gastropods", *Journal of Experimental Biology*, vol. 213, no. 22, pp. 3920-3933, 2010.

[6] **R. Dubois and F.Vles**, "Locomotion des Gasteropodes", pp. 658-659, 1907.

[7] **E. Lauga and A. Hosoi**, "Tuning gastropod locomotion: Modeling the influence of mucus rheology on the cost of crawling", *Physics of Fluids*, vol. 18, no. 11, p. 113102, 2006.

[8] **H.W. Lissmann**, "The mechanism of locomotion in gastropod molluscs", *Journal of Experimental Biology*, no. 22, pp. 58-69, 1945

[9] **M. Denny**, "Locomotion: The Cost of Gastropod Crawling", *Science*, vol. 208, no. 4449, pp. 1288-1290, 1980.

[10] **M. Davies, S. Hawkins and H. Jones,** "Mucus production and physiological energetics in Patella Vulgata L.", *Journal of Molluscan Studies*, vol. 56, no. 4, pp. 499-503, 1990.

[11] **A. Kideys and R. Hartnoll**, "Energetics of mucus production in the common whelk Buccinum undatum L.", *Journal of Experimental Marine Biology and Ecology*, vol. 150, no. 1, pp. 91-105, 1991.

[12] **M. Denny**, "Mechanical Properties of Pedal Mucus and Their Consequences for Gastropod Structure and Performance", *American Zoologist*, vol. 24, no. 1, pp. 23-36, 1984.

[13] **G. Parker**, "The mechanism of locomotion in gastropods", *Journal of Morphology*, vol. 22, no. 1, pp. 155-170, 1911.
[14] H. Jones, "The mechanism of locomotion of Agriolimax reticulatus (Mollusca: Gastropoda)", *Journal of Zoology*, vol. 171, no. 4, pp. 489-498, 2009.

[15] **M. Denny**, "The role of gastropod pedal mucus in locomotion", *Nature*, vol. 285, no. 5761, pp. 160-161, 1980.

[16] **J. Lai, J. del Alamo, J. Rodriguez-Rodriguez and J. Lasheras**, "The locomotion of marine and terrestrial gastropods: can the acceleration of the ventral pedal waves contribute to the generatin of net propulsive forces? ", *Researchgate,* 2008.

[17] **A.J. Perez Vidal**, "Desarrollo de un Sistema PIV (velocímetro por imagen de partículas) didáctico ", Dissertation, Dpt. of Applied Physics, Universidad Politécnica de Valencia, Valencia, España, 2016. [online]. Available at: https://riunet.upv.es/bitstream/handle/10251/75809/P%C3%89REZ%20-%20DESARROLLO%20DE%20UN%20SISTEMA%20PIV%20%28VELOCIMETRO%20POR%20IMAGEN%20DE%20PART%C3%8DCULAS%29%20DID%C3%81CTICO.pdf?sequence=1). [Accesed: 12 Sep-2018].

[18] **M. Watanabe and H. Tsukagoshi,** "Suitable configurations for pneumatic soft sheet actuator to generate traveling waves", *Advanced Robotics*, vol. 32, no. 7, pp. 363-374, 2017.

[19] **T. Nakamura and K. Satoh**, "Development of an omni- directional mobile robot using traveling waves based on snail locomotion", *Industrial Robot: An International Journal*, vol. 35, no. 3, pp. 206-210, 2008.

[20] NRC [National Research Council] .2011. Guide for the Care and Use Of Laboratory Animals, 8th ed. Washington, DC : T*he National Academies Press*. p 220.

[21] "Experiments on Invertebrate Animals — DRZE", Drze.de, 2018. [Online]. Available: http://www.drze.de/in-focus/animal-experiments-in-

research/modules/experiments-on-invertebrate-animals?set_language=en.   [Accessed: 12- Sep- 2018].

[22] "USDA APHIS | Snails and Slugs", Aphis.usda.gov, 2018. [Online]. Available: https://www.aphis.usda.gov/aphis/ourfocus/planthealth/import-information/permits/regulated-organism-and-soil-permits/sa_snails_slugs/ct_snails_slugs. [Accessed: 12- Sep- 2018].

[23] **M. Jahanmiri**, " Particle Image Velocimetry: Fundamentals and Its Applications", 2011.[Online].Available: https://pdfs.semanticscholar.org/019f/d4139e6e3b99784eda8f5af23a9cfd3be295.pdf. [Accessed: 12- Sep- 2018].

[24] "Advanced PIV analysis algorithms | SEIKA DIGITAL IMAGE CORPORATION", Seika-mt.com, 2018. [Online]. Available: http://www.seika-mt.com/product/piv-en/PIV_software_Koncerto-02.html. [Accessed: 12- Sep- 2018].

[25] **J. Perona, M. González, M. Romero, L. Moreno and J. Jiménez**, "Índice de complejidad y análisis de los costes de las endoscopias digestivas en un hospital universitario", *Gastroenterología y Hepatología*, vol. 25, no. 2, pp. 71-78, 2002.

[26] "El uso de la endoscopia crecerá un 7% anual hasta 2021", infosalus.com, 2018. [Online]. Available: http://www.infosalus.com/asistencia/noticia-uso-endoscopia-crecera-anual-2021-20151120113853.html. [Accessed: 12- Sep- 2018].

[27] **A. McKee, J. Voltzow and B. Pernet**, "Substrate Attributes Determine Gait in a Terrestrial Gastropod", *The Biological Bulletin*, vol. 224, no. 1, pp. 53-61, 2013.

[28] **M. Iwamoto, D. Ueyama and R. Kobayashi**, "The advantage of mucus for adhesive locomotion in gastropods", *Journal of Theoretical Biology*, vol. 353, pp. 133-141, 2014.

[29] "Leopard Slug - Limax maximus - Details - Encyclopedia of Life", Encyclopedia of Life, 2018. [Online]. Available: http://eol.org/pages/452590/details. [Accessed: 21- Sep- 2018].